Microrefugia and microclimate: Unraveling decoupling potential and resistance to heatwaves

Marie Finocchiaro, Frédéric Médail, Arne Saatkamp, Katia Diadema, Daniel Pavon, Lenka Brousset, Eric Meineri

Microrefugia and microclimate: Unraveling decoupling potential and resistance to heatwaves

Marie Finocchiaro, Frédéric Médail, Arne Saatkamp, Katia Diadema, Daniel Pavon, Lenka Brousset, Eric Meineri

PII: S0048-9697(24)01838-2

DOI: https://doi.org/10.1016/j.scitotenv.2024.171696

Reference: STOTEN 171696

To appear in: *Science of the Total Environment*

Received date: 15 November 2023

Revised date: 11 March 2024

Accepted date: 11 March 2024

Please cite this article as: M. Finocchiaro, F. Médail, A. Saatkamp, et al., Microrefugia and microclimate: Unraveling decoupling potential and resistance to heatwaves, *Science of the Total Environment* (2023), https://doi.org/10.1016/j.scitotenv.2024.171696

Microrefugia and microclimate: unraveling decoupling potential and resistance to heatwaves

Marie Finocchiaro[1], Frédéric Médail[1], Arne Saatkamp[1], Katia Diadema[2], Daniel Pavon[1], Lenka Brousset[1], Eric Meineri[1]

[1]Aix Marseille Université, Université Avignon, CNRS, IRD, UMR IMBE, Marseille, France.

[2]Conservatoire botanique national méditerranéen, 34 avenue Gambetta, F-83400 Hyères, France.

Corresponding author: Marie Finocchiaro - marie.finocchiaro@hotmail.com

Abstract

Microrefugia, defined as small areas maintaining populations of species outside their range margins during environmental extremes, are increasingly recognized for their role in conserving species in the face of climate change. Understanding their microclimatic dynamics becomes crucial with global warming leading to severe temperature and precipitation changes. This study investigates the phenomenon of short-term climatic decoupling within microrefugia and its implications for plant persistence in the Mediterranean region of southeastern France. We focus on microrefugia's ability to climatically disconnect from macroclimatic trends, examining temperature and Vapor Pressure Deficit (VPD) dynamics in microrefugia, adjacent control plots, and weather stations. Our study encompasses both “normal” conditions and heatwave episodes to explore the role of microrefugia as thermal and moisture insulators during extreme events. Landscape attributes such as relative elevation, solar radiation, distance to streams, and vegetation height are investigated for their contribution to short-term decoupling. Our results demonstrate that microrefugia exhibit notable decoupling from macroclimatic trends. This effect is maintained during heatwaves, underscoring microrefugia's vital role in responding to climatic extremes. Importantly, microrefugia maintain lower VPD levels than their surroundings outside and during heatwaves, potentially mitigating water stress for plants. This study advances our understanding of microclimate dynamics within microrefugia and underscores their ecological importance for plant persistence in a changing climate. As heatwaves become more frequent and severe, our findings provide insights into the role of microrefugia in buffering but also decoupling against extreme climatic events and, more generally, against climate warming. This knowledge emphasizes the need to detect and protect existing microrefugia, as they can be integrated into conservation strategies and climate change adaptation plans.

Keywords: Refugia; Temperature; Vapor Pressure Deficit; Extreme events; Climate Change; Mediterranean Basin.

1. Introduction

With global warming, many species face unprecedented challenges to cope with rapidly changing environmental conditions (Jump & Peñuelas, 2005; Parmesan & Hanley, 2015; Pecl et al., 2017). The resulting changes in temperature and precipitation patterns affect ecosystems worldwide, profoundly impacting species distribution and persistence (Chen et al., 2011; IPCC, 2023). Rear-edge populations of temperate and arid biomes, living close to their warm limits of distribution, are threatened by rising temperatures and drier conditions and are especially vulnerable to extinction (de Medeiros et al., 2018; Kuhn & Gégout, 2019; Kolzenburg, 2022; Cartereau et al., 2023). Heatwaves, periods with several days of excessively hot weather, and their forecasted intensification exacerbate the situation (Meehl & Tebaldi, 2004). They induce drastic short-term increases in temperatures and Vapor Pressure Deficit (VPD), accelerating evapotranspiration rates and reducing soil moisture (Miralles et al., 2019). Those extremes and more frequent events result in significant increases in water stress for plants, raising their vulnerability to global changes (Dusenge et al., 2019; Notarnicola et al., 2021; Breshears et al., 2021).

Microrefugia are defined as small areas sustaining populations of species outside their range margins during periods of environmental stress (Parducci et al., 2012). Their potential in conserving populations during climatic changes has received increasing attention from researchers (Rull, 2010; Finocchiaro et al., 2023), but their precise role and inner mechanism during the upcoming climate warming and heatwaves are not yet well understood (Gentili et al., 2015; Lenoir et al., 2017). This mechanism is assumed to depend on specific microclimatic conditions that differ from the surrounding landscape (Rull, 2009; Hannah et al., 2014). Previous research has shown that these microsites experience a colder microclimate than the immediate surrounding environment (Finocchiaro et al., 2023; Frei et al., 2023). This absolute temperature difference has been described as the "buffering effect" (Dobrowski, 2011; Lenoir et al., 2013; Thorne et al., 2023). Multiple landscape features are suggested for providing buffered microclimatic conditions, such as concave relief patterns, proximity

to water bodies, or the density of vegetation cover (Scherrer & Körner, 2011; Meineri et al., 2015; Greiser et al., 2018; Zellweger et al., 2020). However, these features may not be sufficient to ensure long-term population persistence in the face of the current pace and magnitude of climate change.

The ability of microrefugia to shelter species threatened by climate change may also depend on a reduced correlation to regional climate fluctuations within the microrefugia (Dobrowski, 2011; Keppel et al., 2012; Hylander et al., 2015). This phenomenon, known as the "decoupling effect," is characterized by a decorrelation between the microclimate of microrefugia and the surrounding macroclimate (Lenoir et al., 2017; De Frenne et al., 2021). The "decoupling effect" is necessary for microrefugia to function effectively as a refugium in the long term, i.e., preserving populations they host from the adverse effects of climate change (Hylander et al., 2015). However, despite their pivotal role, empirical evidence validating decoupling processes within microrefugia remains rare, possibly due to the limited and recent monitoring of such sites (Nadeau et al., 2022; Finocchiaro et al., 2023). While long-term monitoring of climate, fauna, and flora (over a decade) is necessary to demonstrate the existence and effectiveness of decoupling processes within microrefugia (Dobrowski, 2011), short-term investigations (at the day or week scale) can inform on the immediate potential of microrefugia to mitigate the effects of climatic extreme events (Aalto et al., 2018). This immediate response, which we will hereafter term “short-term decoupling”, becomes particularly relevant in the face of intensifying heatwaves, which are both more frequent and severe (Chapman et al., 2019) and may increase the climatic vulnerability of such sites (Keppel et al., 2023). Microrefugia with a high degree of short-term decoupling may effectively preserve their microclimatic specificity and the species they shelter, even during intensifying climatic extreme events.

Incorporating moisture-related parameters, such as Vapor Pressure Deficit (VPD), into the examination of microrefugia may also offer a deeper understanding of microclimatic conditions experienced by plants. The importance of VPD in influencing plant water balance through transpiration and its potential impact on microclimate regulation has been identified before (Ashcroft & Gollan, 2013; Grossiord et al., 2020). By examining VPD, we can increase our understanding of how microrefugia's climate influences plant persistence under changing environmental conditions.

During phases of high VPD leading to extreme water losses in plants, microrefugia might offer suitable environments for plants by maintaining lower VPD (Yuan et al., 2019; Sanginés de Cárcer et al., 2018).

Our objective is to examine the occurrence of short-term microclimatic decoupling within microrefugia by studying the correlations between temperatures measured (i) within microrefugia, (ii) in the immediate vicinity, and (iii) at nearby weather stations that reflect regional conditions. We specifically ask to which degree the microrefugia temperatures are decoupled from the temperatures in the extended landscape and which environmental features can explain those differences. Accordingly, we aim to investigate whether this effect is amplified or mitigated during episodes of heatwaves. If decoupling is present in current microrefugia, it may become more pronounced during heatwaves when macroclimatic fluctuations peak. Moreover, as we recognize that factors beyond temperatures can significantly influence microrefugia climatic regimes, we will also investigate potential buffering and decoupling processes of VPD in microrefugia. Since high VPD indicates dry conditions where moisture is being pulled from plants more quickly, potentially leading to water stress, we hypothesize that VPD is buffered and decoupled in microrefugia compared to the surroundings so that plants are under less stress from water loss.

To answer these questions, we have set up microclimatic monitoring of the most meridional marginal populations in southeastern Mediterranean France of two plant species with a large mid-European distribution (*Oxalis acetosella* L. and *Arabis alpina* L.). These populations are suspected to indicate current microrefugia since they occur beyond the warm edge of the species distribution, in areas with unfavorable macroclimate (Rull, 2009). Quantifying the degree of short-term decoupling of microrefugia already sheltering them and understanding the underlying mechanisms involved in these processes will help to evaluate microrefugia's capacity for long-term conservation of plant persistence.

2. Materials and methods

2.1. Study area

The study was conducted in the "*Région Provence, Alpes, Côte d'Azur"* (PACA region), extending across 31 400 km² in southeastern France, characterized by a Mediterranean climate with hot, dry summers and mild winters, i.e., the most widespread climate type corresponding to Csb and Cfb according to Köppen classification (Köppen, 1900). Mean annual temperatures are remarkably contrasted throughout the region, ranging from -8 °C in its northern part in the Alps to 18°C in Provence. Precipitations mainly occur during autumn and winter, with important inter-annual variations and contrasting local precipitation, from 500 mm in its western part to 1400 mm in the northern Mediterranean mountains (Vignal, 2020; Météo France, 2023). Biogeographically, this region is located at the transition between Mediterranean, mountainous, and alpine ecosystems. This unique position has contributed to the region's rich biodiversity, and its topography, including canyons and mountain ranges, contributes to the unique landscape diversity of this regional biodiversity hotspot (Médail & Quézel, 1997). From Mediterranean pine and oak forests to alpine meadows and mountain habitats, the region showcases a wide array of forest ecosystems, covering almost half the surface of the area. This rugged topography and highly diverse forests offer remarkable microclimate gradients that may favor the presence of numerous microrefugia (Harrison & Noss, 2017; Aurelle et al., 2022). As part of the Mediterranean Basin, this region is also particularly exposed to the consequences of global warming, as it is highly exposed to intensifying heatwaves and droughts (Fischer & Schär, 2010; Gouveia et al., 2017). It is predicted to experience a hotter and drier climatic regime, especially during summers (> +3°C in temperature and -10% in precipitation, following the Representative Concentration Pathway 8.5, representing a "business as usual" scenario of emissions), with an intensification of droughts periods and longer and archer heatwaves, impacting the spatial distribution of living organisms (MedECC, 2020).

2.2. Studied putative microrefugia

In our study, we assimilated the southernmost disconnected and abyssal (i.e., at an exceptionally low elevation) populations of *Oxalis acetosella* L. (Oxalidaceae) and *Arabis alpina* L. (Brassicaceae), both at their warm-edge limits in the study region, as putative microrefugia, as described in Finocchiaro et al. (2023).

Oxalis acetosella is a geophytic forest herb with a circumpolar distribution, primarily occurring in temperate and boreal biomes (Rameau et al., 1989). It predominantly occurs between 1200 and 2000 m, often in shaded habitats with a dense tree canopy and low luminosity (Rameau et al., 1989). *Arabis alpina* is a chamaephyte herb with an artico-alpine distribution, ranging up to 3000 m in the Alps. It is primarily found in mountainous regions of Europe, in alpine meadows, rocky slopes, and screes, with a preference for calcareous soils and sunny or partially shaded locations (Rameau et al., 1989).

The selection of putative microrefugia followed a three-step process. First, we identified sites where either species occurred below their respective 5th percentile of the altitudinal range in the region (specifically, <1018 m for *Oxalis acetosella* and <1080 m for *Arabis alpina*). Second, we selected sites based on their isolation, with the nearest high-altitude neighboring individuals located at least 500 m vertically and horizontally away. Thirdly, we refined the selection of populations by retaining only the southernmost populations within each species, resulting in 30 study sites—20 for *Arabis alpina* and 10 for *Oxalis acetosella* (**Fig.1**)**.** The occurrence data for both species were sourced from the SILENE-Flore database (CBNMed & CBNA, 2019), utilizing only georeferenced records with a minimum resolution of 10 m.

To enhance statistical power and understand microrefugia functionality, distinct putative microrefugia for each of the two studied species were investigated simultaneously. This approach increases the number of observations and allows for a broader understanding of microrefugia functioning, irrespective of the species they shelter, as microclimatic processes are expected to be similar. The population selection process, which involves the identification of low-elevation and isolated populations, was carried out using ArcMap (ESRI, 2020)**.**

2.3. Micro- and macroclimatic measurements

To study the short-term decoupling processes between microrefugia and the surrounding landscape, we recorded climate in two distinct plots within each site: a microrefugium plot where the target species was present and a control plot located 50 to 100 m away where the species was absent. The control plots were systematically located with a northern aspect and higher elevation to serve as

reference points, a conservative choice to enhance our ability to identify colder climatic conditions within microrefugia that are not solely attributed to the typical variations associated with altitude and exposition. In each plot, TOMST thermologgers were placed at 1.5 m above the ground to monitor temperatures every 15 minutes, and humidity sensors (Lascar USB-2) were placed under a protection shield at a 30 cm height, recording the percentage of relative air humidity each hour. Finally, we selected the nearest weather station from the national meteorological web "Météo-France", at a distance of 10 km (±3,54) on average (**Annex 1**), which monitors both daily air temperatures and humidity, representing macroclimatic trends. National weather stations are strategically positioned in flat terrain with no canopy cover to minimize the influence of local landscape on climatic measures. A schematic view of the relative position and characteristics of individual plots on a site can be found in the graphical abstract.

The monitoring of temperatures extends from September 2021 to October 2022, an exceptionally arid and warm period in the region, with a precipitation deficit of -30% and +3.3°C of maximum temperature anomalies compared to the period 1961-1990, the year 2022 breaking the record of the warmest year ever recorded in the area (GREC-SUD, 2023). To gain a comprehensive understanding of the thermal variability in these sites, we computed the 5th percentile of daily minimum temperatures (T_{Min}), the 95th percentile of daily maximum temperatures (T_{Max}), and the daily mean temperatures (T_{Mean}) for each microrefugium plot, control plot, and the nearest weather station. In addition, we also computed the daily mean, 95th percentile of daily maximum, and the 5th percentile of daily minimum vapor pressure deficit (respectively, VPD_{mean}, $VPD_{max,}$ *and* VPD_{min} in hPa) for each plot. VPD was computed following the same methodology of VPD calculation as in Jucker et al. (2018), considering the interplay between temperature (T) and relative humidity (RH) :

$$VPD = [(100 - RH)/100] \times e_s$$

where e_s, the saturation water vapor pressure, is derived from temperature (T) using Bolton's (1980) equation:

$$e_s = 6.112 \times e^{\frac{17.67 \times T}{T+243.5}}$$

2.4. Heatwave detection

As we aim to explore whether a current short-term decoupling effect within microrefugia is accentuated or alleviated during episodes of heatwaves, a critical step is to detect when those events are occurring at each monitored site. Heatwaves are characterized by a period of hot weather, typically lasting two or more days, with temperatures surpassing a threshold or a percentile of the distribution of a 30-year reference period over three to five days (Perkins & Alexander, 2013). In the context of our study area, we adapted a heatwave identification method developed by the French national weather agency *Météo-France* in 2006 (Soubeyroux et al., 2016).

We first extracted daily temperature records from the Météo-France database for weather stations in our study region that had 30 years of operational daily data during the current reference climate period spanning from 1991 to 2020 (Sorel et al., 2022), and that also operated during our study period, resulting in 42 weather stations. Such a historical dataset makes it possible to identify abnormal temperature fluctuations. Using the data from each selected station, we computed its daily average air temperature based on its specific 30-year reference period measurements. Then, to detect heatwaves, our method uses two key parameters: (i) a 99.5th percentile heat peak threshold to identify significant heat events (*Spic*); and (ii) a 97.5th percentile start and end threshold to determine the onset and the end of a heatwave (*S*). Additionally, each heatwave must correspond to a period during which the threshold *S* was reached for at least three days and the threshold *Spic* was reached at least once. This allowed us to identify heatwave events occurring in each weather station of the region during the study period. For each site, we reported the heatwave events detected in the three nearest weather stations of reference to the closest microrefugia, their control plots, and their nearest weather stations. This methodology ensures a comprehensive and spatialized analysis of heatwave occurrences, enabling us to investigate the potential exacerbation of short-term decoupling processes between microrefugia and the surroundings (**Fig.2**). While winter and fall heatwaves may occur more often in the future, we choose to focus on spring and summer heatwaves for this study, as they are typically the seasons when heatwaves are predicted to have the most significant ecological impact.

We identified 57 heatwaves occurring locally during spring and summer—11 in spring and 46 in summer. On average, each site experienced approximately seven heatwaves (6.7 with a standard deviation of 1.7), lasting 4.65 days (±0.52).

2.5. Airborne laser scanning data and derived microclimatic forcing factors

The use of Aerial Laser Scanning (ALS) makes it possible to finely characterize the microclimate forcing factors, which are topographic and forest-related variables that significantly impact the climate at a local scale (Zellweger et al., 2019). To estimate the forcing factors influencing short-term decoupling in microrefugia, we utilized raw Light Detection and Ranging data (LiDAR) data, available in open access through the French National Institute of Geographic and Forestry Information (LiDAR HD - IGN), with a mean point density of 10 pulses/m² and 5 pulses/m² above 3200 m (LiDAR HD, 2023). Each available file was cropped to several areas of interest, corresponding to a 600 m buffer zone around the GPS coordinates of each microrefugium, control plot, and nearest weather station. The mean point density for those files reached 23 pulses/m² (37 points/m²). Subsequently, point clouds were classified using a Multiscale Curvature Classification (MCC) algorithm, enabling us to extract 1m-resolution Digital Terrain Models (DTMs) for each site through a kriging algorithm.

From these DTMs, we computed specific topographic variables per microrefugium, control plot, and weather station, known to influence microclimate, based on existing literature (Dobrowski, 2011; Meineri et al., 2015). Firstly, we extracted the relative elevation within a 500 m radius, as it serves as a proxy for cold air drainage, favoring microclimatic conditions for microrefugia (Ashcroft & Gollan, 2012; Pastore et al., 2022). Additionally, we used the distance to the nearest stream section (BD TOPO Hydrography 2019; IGN), as it acts as a temperature buffer (Meineri et al., 2015; Meineri & Hylander, 2017). Lastly, we computed incoming solar radiation at each plot based on methods from the hemispherical viewshed algorithm (Fu & Rich, 2002).

To study the influence of vegetation parameters, we cropped each classified point cloud to a 10 m radius zone around each microrefugium, control plot, and weather station. These point clouds were

then normalized using a k-nearest neighbor approach with inverse-distance weighting, followed by removing outliers. This preprocessing allowed us to compute three vegetation-related variables based on methods described in Moudrý et al. (2022): (i) the canopy cover (expressed as a percentage), which describes the proportion of the ground covered by vegetation; (ii) the standard deviation of vegetation height of trees (in meters), indicating vertical variability and providing insight into the inner vegetation structure and strata levels within the plot; (iii) the mean vegetation height (in meters), representing the average height of vegetation within the plot.

The processing of LiDAR data and computation of forestry variables were conducted in R (version 4.1.1) using the lidR package (Roussel et al., 2020). The lidR package was employed to process the raw LiDAR data, classifying the data, extracting 1m-resolution DTMs with the kriging() method from the gstat package (Gräler et al., 2016), and normalize the point clouds. Furthermore, ArcGIS Pro software (version 2.8) was used to extract topographic variables from each 1m-resolution DTM.

2.6. Statistical analysis

Coupling and decoupling mechanisms permit to describe a site's climatic regimes in reference to another, usually microclimatic regimes of a site compared to the macroclimate (**Fig.3a**). De Frenne et al. (2021) propose to study coupling and decoupling processes by examining the regression slope β_1 of the linear relationship between temperatures inside and outside microrefugia (**Fig.3b**). A slope of 0 indicates a total decoupling capacity, where temperatures inside microrefugia behave independently of external conditions (Site B in **Fig.3a and Fig.3b**). Conversely, a slope of 1 indicates a perfect coupling, representing a strict correlation between both climatic regimes (Site A in **Fig.3a and Fig.3b**). Finally, slopes between 0 and 1 illustrate various degree of (de)coupling. However, regression models test if β_1 differs from 0, not from 1. In other words, by modeling the microclimate against the macroclimate, models test for a significant deviation from a perfect decoupling situation.

In our context, we want to test if sites' microclimates exhibit a significant decoupling from macroclimate. Therefore, we tested the level of decoupling between sites and macroclimate through a linear regression analysis, where the difference in temperature between the sites' microclimate and

macroclimate was used as the response variable and the temperature of the macroclimate was used as explanatory variable (**Fig.3c**). By doing so, the p-value associated with the regression slope of the model (β_1) tests whether the difference in temperature between sites and macroclimate change as macroclimate temperature increases or decreases. In these models, a slope equal to 0 indicates a perfect coupling, i.e., the temperature difference between sites and macroclimate remains identical regardless of macroclimate temperatures (Site A in **Fig.3c**). On the contrary, a significant negative slope indicates that the difference in temperature between sites microclimate and the macroclimate increases as temperature becomes higher at a macro scale and the temperatures at the site scale remain stable and lower, meaning a decoupling of temperature (Site B in **Fig.3c**).

We conducted linear mixed models to test the short-term temperature decoupling capacity of microrefugia throughout the study period by (i) regressing temperature differences between microrefugia and control plots against temperatures in control plots and (ii) regressing temperature differences between each microrefugia and the nearest weather station against the temperatures in the nearest weather station. The analyses were based on daily temperature data. We also explored the capacity of short-term decoupling for control plots compared to the nearest weather station using the same method. All models were fit with Restricted Maximum Likelihood (REML), with species of interest and sites as nested random terms to account for spatial correlation. We also incorporated the corAR1(form = ~ Date | Species/Site) variance structure to address temporal autocorrelation.

To identify microclimate forcing factors influencing the degree of climatic decoupling in microrefugia, we calculated the degree of decoupling of mean, maximum, and minimum temperatures for each site, using individuals Generalized Least Squares (GLS) models using the same method as the models described in the previous paragraph. We extracted the slope parameter of each of these models as it indicates the degree of climatic decoupling. This was done for the degree of decoupling between microrefugia and weather station and between microrefugia and control. All GLS models include a corAR1 variance structure to address temporal autocorrelation. The degrees of decoupling extracted for each site were then regressed against topographic and forest-related variables in the following way. A first model assessed the degree of decoupling between microrefugia and weather stations against the

differences in topographic variables (termed "delta" hereafter) of relative elevation, incoming solar radiation, and distance to the nearest stream section between the same two sites, along with forest-related variables within the microrefugia. We did not consider deltas for forest variables due to the absence of forests in weather stations. A second model examined the degree of decoupling between control plots and microrefugia against the same potential forcing factors variables. Both topographic and forest-related features were considered deltas since control plots included vegetation cover. These models were fitted for the decoupling of mean, minimum, and maximum temperatures. A stepwise selection was conducted for both sets of models to identify the most influential variables and derive the best-fitting models. The environmental features used here were derived from LiDAR data, as detailed in **section 2.5**. In these models, a negative estimate signifies that the decoupling of temperatures between microrefugia and weather station, or control plots, increases when the difference in topographic and forest forcing factors between the same two types of plots increases. This analysis spanned the entire study period. The degree of decoupling of mean, maximum, and minimum temperatures for each site can be found in **Annex 3** and **Annex 4** for the decoupling of microrefugia to weather stations and to control plots, respectively.

Similar linear mixed models were performed to assess the impact of spring and summer heatwaves on short-term decoupling processes but included heatwave periods as a covariable. The models used the differences of daily temperatures in microrefugia, first against the temperature recorded in control plots, and then against the temperature recorded in nearest weather stations, and also included the period of heatwaves (coded as 1 during a period of heatwaves and 0 otherwise) and its interaction with daily air temperatures in the surrounding sites (control plots or nearest weather stations) as explanatory variables. These models were conducted using a reduced dataset, focused on temperatures in microrefugia, control plots, and nearest weather stations 10 days before each heatwave, the heatwave period, and 10 days after each heatwave (green arrows and red area in **Fig.2**), to specifically examine climatic regimes during these extreme events. Detailed results of the models can be found in **Annex 5**.

To uncover patterns of VPD contrasts between microrefugia and their surroundings, separate linear mixed-effects models were constructed for mean, maximum, and minimum VPD in microrefugia, first against VPD in control plots and then against VPD in nearest weather stations. We performed these models on the reduced dataset from 10 days before to 10 days after each heatwave (green arrows and red area in **Fig.2**) and informed sites as random effects. Finally, *post hoc* pairwise comparisons between plot types within different heatwave periods were conducted. This analysis aimed to identify an offset of VPD between microrefugia and surroundings during heatwave and non-heatwave periods.

Finally, to assess the impact of spring and summer heatwaves on VPD decoupling processes, we performed linear mixed models using the differences of daily VPD in microrefugia, first against the VPD recorded in control plots and then against the VPD recorded in nearest weather stations, and also included the period of heatwaves and its interaction with daily VPD in the surrounding sites (control plots or nearest weather stations) as explanatory variables. Similar to temperature decoupling modeling, these models were conducted using a reduced dataset, focused on VPD in microrefugia, control plots, and nearest weather stations, 10 days before each heatwave, the heatwave period, and 10 days after each heatwave (green arrows and red area in **Fig.2**). Results of the models can be found in **Annex 8**.

All statistical analyses were conducted in R (version 4.1.1). The nlme package (Pinheiro & Bates, 2023) was used to fit all mixed effects and GLS models, and the package emmeans (Russell, 2021) was used to perform *posthoc* tests.

3. Results

3.1. Degree of short-term decoupling in microrefugia

During the entire study period (September 2021 to October 2022), we consistently observed significant differences in climatic regimes between microrefugia and both control plots and nearest weather stations, based on mixed effect linear regression analysis (**Table 1**). The degree of short-term decoupling between microrefugia and the nearest weather station is quite strong, approaching – 0.5 for

all temperature metrics ($p<0.001$), meaning that for a variation of 1°C at the weather station, only 0.5°C would be detected in the microrefugium (dotted lines in **Fig.4**). The degree of decoupling between microrefugia and control plots are also significant for the mean (-0.154, $p<0.001$), maximum (-0.226, $p<0.001$), and minimum (-0.037, $p<0.001$) temperatures (full line in **Fig.4**). Finally, the temperatures in control plots are decoupled from weather stations, but to a lesser extent than microrefugia (**Table 1**).

3.2. Topography, forest structure, and short-term decoupling

Concerning the decoupling between microrefugia and weather stations (upper part of **Table 2**), the analysis reveals that an increasing difference in relative elevation between microrefugia and weather station leads to a higher decoupling for mean temperatures (-0.114, $p < 0.01$, **Table 2**). Moreover, increased differences in incoming solar radiation, as well as higher vegetation height in microrefugia, result in amplified maximum temperature decoupling (-0.073 and -0.113 respectively, $p < 0.01$), both variables explaining 64% of the total variance of the model (**Table 2**). Finally, none of the variables significantly explained minimum temperature decoupling between microrefugia and weather stations.

The decoupling of mean temperatures between microrefugia and control plots significantly decreased with the difference in the standard deviation of tree height (0.061, $p = 0.015$), implying that a greater vertical heterogeneity in vegetation within control plots, compared to microrefugia, led to a reduction in temperature decoupling between the sites. The decoupling of maximum temperature increased as more solar radiation was received in control plots than in microrefugia (-0.106, $p = 0.018$). Finally, the degree of decoupling of minimum temperatures increased significantly when microrefugia were closer to the nearest stream section (-0.052, $p = 0.009$).

3.3. Impact of heatwaves on climatic short-term decoupling

Compared to their respective nearest weather stations, outside heatwaves (in green in **Fig.5a)**, the degree of short-term decoupling of microrefugia is strong and significant for all temperature metrics ($p<0.001$), which is concordant with previous results for the whole study period in section 3.1.

During heatwave events (in red in **Fig.5a**), the decoupling process increases almost significantly for mean temperatures ($p = 0.056$) but with a marginal effect otherwise. This suggests that the temperature decoupling between microrefugia and the nearest weather stations is slightly but not significantly exacerbated during heatwave events.

When comparing microrefugia to their respective control plots outside heatwaves, namely 10 days before and 10 days after each heatwave (**Fig.5b**), the results suggest that the temperatures inside microrefugia significantly decoupled from temperature patterns observed in the control plots ($p<0,001$ for mean, minimum and maximum temperature), which is once again concordant with previous results during the whole study period of section 3.1. During heatwave events, the decoupling effect significantly increases ($p<0.05$).

3.4 Humidity trends during and outside heatwaves

Applying linear mixed models and *posthoc* tests on Vapor Pressure Deficit (VPD) metrics, we found significantly lower VPD (higher moisture) in microrefugia compared to their surroundings. VPD was lower both during heatwaves and in non-heatwave periods (**Fig.6**, details from the linear mixed models and Tukey *posthoc* tests are available in **Annexes 6 and 7**).

The nearest weather stations exhibit a higher VPD than microrefugia (mean offset of 3.603 hPa, 1.634 hPa, 3.939 hPa for mean, minimum and maximum VPD, respectively, $p < 0.001$). During heatwaves, these offsets notably increase to 4.542 hPa, 1.969 hPa, and 5.657 hPa for mean, minimum, and maximum VPD, respectively ($p<0.001$). These results suggest a systematic higher moisture into microrefugia, exacerbated during heatwaves. Similarly, outside heatwave periods, VPD is systematically higher in control plots compared to microrefugia (offset of 2.695 hPa, 1.006 hPa, and 4.893 hPa, for mean, minimum, and maximum VPD respectively, $p < 0.001$). These offsets also significantly increase during heatwaves to 3.018 and 5.672 hPa ($p<0.001$) for mean and maximum VPD, respectively. Last, the offsets between the nearest weather stations and control plots suggest a lower mean (0.908 hPa, $p <0.01$) and minimum VPD (0.629 hPa, $p<0,001$) in control plots, and the

models indicate that these offsets increase during heatwaves (1.523 hPa and 0.891 hPa respectively, p<0,001).

3.5. VPD decoupling outside and during heatwaves

Outside heatwave periods, the degree of short-term decoupling of microrefugia compared to their respective nearest weather stations is strong for mean, minimum, and maximum VPD (in green in **Fig.7a**, p<0.001). During heatwave events, the decoupling process is still significant for all three metrics, and increases significantly for mean and maximum VPD (in red in **Fig.7a**, $p < 0.05$), with a marginal effect for minimum VPD (p= 0.243).

Outside heatwave periods, our results suggest that mean, minimum, and maximum VPD inside microrefugia are significantly decoupled from VPD patterns observed in the control plots (in green in **Fig.7b**, p<0,001). These decoupling effects significantly decrease during heatwave events for mean and minimum VPD (in red in **Fig.7b**, p<0.05).

4. Discussion

In this study, we focused on short-term decoupling dynamics and revealed the inherent ability of microrefugia's microclimate to decouple from its surroundings. Although our observations span one year, our findings suggest that microrefugia could serve as stable and moister enclaves, even during the warmest year ever recorded in the region.

4.1. Decoupling capacity of microrefugia and the role of microclimatic forcing factors

Temperatures inside microrefugia are characterized by a significant short-decoupling from temperature patterns observed in the adjacent control plots. The degree of decoupling between microrefugia and their respective nearest weather stations was even more pronounced. Investigating the microclimate forcing factors influencing the decoupling effect can provide answers to explain those differences.

The degree of decoupling of mean temperatures between microrefugia and weather stations exhibited a significant negative association with greater differences in relative elevation. These

findings align with well-documented processes, where sites located at low elevations compared to the surroundings are known to accumulate cold air and to experience temperature inversions favoring temperature decoupling (Lookingbill, 2003; Lundquist et al., 2008; Meineri & Hylander, 2017). The pronounced impact of this topographic variable on mean temperature decoupling underscores its role in creating microhabitats with distinct thermal regimes, effectively sheltering plant communities from the temperature fluctuations of the broader landscape (Pastore et al., 2022). Additionally, mean vegetation height in microrefugia significantly increases the decoupling of maximum temperatures between microrefugia and weather stations: microrefugia with higher vegetation have temperatures that are more decoupled from the macroclimate (Jucker et al., 2018). Lastly, our estimation of incoming solar radiation does not consider the forest layer, yet we found a significant negative relationship between increased differences in incoming solar radiation and temperature decoupling of maximum temperature. This pattern holds the temperature decoupling between microrefugia and weather stations and also between microrefugia and control plots. It implies that sites receiving lower solar energy experience independent microclimates, potentially shaping thermal buffers that safeguard plant species from extreme temperature events. Previous studies showed indeed that sites receiving less solar radiation are subject to lower air temperature and humidity (Dobrowski, 2011; Aalto et al., 2017; Słowińska et al., 2022) and that this sheltering participates in thermal decoupling (Keppel et al., 2023; Thorne et al., 2023).

The ability of microrefugia to achieve climatic decoupling from control plots was slightly lower compared to their ability to decouple with the climate recorded at the weather stations. It might be that landscape parameters influencing microrefugia's microclimate extend their impact to a larger spatial scale. Microrefugia and control plots are positioned within 50 to 100 meters of each other, it is, therefore, probable that both plots share common environmental drivers that shape their microclimates. For instance, the difference in relative elevation had no significant effect on the decoupling of mean temperatures between microrefugia and control plots, which may be due to their very close proximity in space (50-100m). The radius of the computed relative elevation being equal to 500m, the delta value for this variable is consequently smaller than with weather stations. In scenarios

where both microrefugia and control plots are situated in deep canyons, microrefugia and control plots may benefit from cold air pooling as one of the common forcing factors. Drawing a parallel, this mechanism echoes the forest microclimate buffering effect, which weakens as one moves away from forest edges, ultimately influencing forest understory conditions (Magnago et al., 2015). Still, the delta of the standard deviation of tree height significantly affected the decoupling of mean temperatures, showing that a higher vertical complexity in microrefugia compared to control plots leads to a higher decoupling. Similarly, DeFrenne et al. (2023) demonstrated that dense vertical layering of vegetation explains colder microclimate under forest cover because of lower moisture exchange and air mixing as well as lower incoming solar radiations. Additionally, the degree of decoupling of minimum temperatures only responded to the vicinity of streams, indicating that microrefugia close to streams have stable and buffered temperature conditions compared to control plots, which are only 50 to 100 m away. This relationship between air and stream temperatures is well-known and has been described before (Meleason & Quinn, 2004; Dan Moore et al., 2005) (Williamson et al., 2021).

We acknowledge that the observed decoupling patterns represent one facet of the complex interplay within sites and might be influenced by yet unexplored microscale factors. Soil composition and depth, moisture and water availability, specificity of foliage cover (deciduous vs coniferous), local vegetation interactions, or landscape features that restrict air movement are just a few examples of additional variables that might interplay to further amplify the decoupling effect (Ashcroft & Gollan, 2013; Cartwright et al., 2020; Pastore et al., 2022). Moreover, landscape features may interact, creating a complex matrix that shapes microclimate behavior (Meineri et al., 2015; Jucker et al., 2018). Understanding the intricate interrelations among these factors and their potential to amplify or counterbalance one another could provide a more comprehensive understanding of the underlying mechanisms governing the microclimate dynamics within microrefugia. The path forward involves a deeper exploration of additional topographic and forest-related features and their intricate interrelations, which may offer novel insights and contribute to a more comprehensive understanding of microrefugia's role in shaping local climate patterns.

4.2. Temperatures decoupling dynamics during heatwaves

Heatwaves exacerbated the existing short-term decoupling effect between microrefugia and adjacent control plots. Thus, the microrefugia's ability to insulate themselves from temperature shifts improves during heatwaves. Microrefugia exhibit a remarkable capacity to maintain distinct microclimates despite rapidly changing external conditions, offering a buffer against temperature-induced plant stress even within proximity.

Examining microclimate dynamics during heatwave events provides a unique lens to dissect the intricacies of decoupling within microrefugia. Heatwaves act as potent magnifying glasses, shedding light on the divergence between microrefugia and their surroundings, thus enhancing our understanding in the face of climatic extremes (Breshears et al., 2021; López et al., 2022; Whalen et al., 2023). Heatwaves reveal the capacity of microrefugia to uphold their distinct climatic conditions. This mitigation capacity underscores the ecological importance of microrefugia as potential havens of stability for organisms, especially plants (Scafaro et al., 2021), but also probably for other taxonomic groups, such as some groups of arthropods (spiders, beetles, ants) or even birds targeting cooler places during the breeding season (Bátori et al., 2022; Ramos et al., 2023).

Our results open avenues for future research. Understanding the interplay of landscape and vegetation attributes in creating decoupled microclimates during heatwaves would enrich our grasp of microrefugia's ecological role (Drake et al., 2018; Wang et al., 2019; Mu et al., 2021). Continuous research monitoring over the long term will be crucial in unveiling the intricacies of this phenomenon (Wolf et al., 2021).

4.3. Vapor Pressure Deficit contribution to microclimate resistance

Besides the fact that VPD increases in all plots during heatwaves (**Annex 4**), microrefugia consistently display lower VPD than control plots and weather stations. This indicates a systematic reduced water stress for plant communities into microrefugia. Higher temperatures lead to increased evaporation rates and, consequently, higher VPD (Grossiord et al., 2020). The fact that microrefugia can maintain lower VPD levels during heatwaves implies their capacity to alleviate temperature-

induced water stress, allowing species to endure high temperatures without experiencing excessive water loss by maintaining a low evaporative demand (Drake et al., 2018; Wang et al., 2019).

We found a significant decoupling of VPD between microrefugia and the surroundings, both with weather stations and control plots, demonstrating the capacity of microrefugia to act as both thermal and humidity insulators for the species they shelter. Notably, this decoupling effect increases during heatwaves compared to the nearest weather stations. This finding further strengthens the role of microrefugia as microclimate refuges, where distinct moisture and temperature levels are maintained independently of surrounding macroclimate trends (Ashcroft & Gollan, 2013). It highlights the role of these sites as buffers and stable refugia against aridity-induced physiological stresses, a characteristic especially important in Mediterranean and more arid bioclimates (Aurelle et al., 2022). The intricate interplay between vegetation structure, moisture availability, hydrological parameters, and microclimate regulation could contribute to the creation of microrefugia that mitigate the impacts of climate warming and extreme events such as heatwaves, enabling easier plant regeneration during drought episodes (Thom et al., 2023).

4.4. Limitations and future avenues

While we successfully demonstrate short-term decoupling of both temperatures and VPD in current microrefugia, we acknowledge the need to investigate decoupling in the long term. This research becomes imperative to understand the persistence and stability of microrefugia under prolonged climatic warming (Wolf et al., 2021). Additionally, future avenues may include investigating the decoupling contrasts between day and night-time. For instance, the impact of landscape features, such as solar radiation or vegetation with evapotranspiration, may differ between day and night, influencing the decoupling of maximum and minimum temperatures (Bennie et al., 2008; Bátori et al., 2019).

Moreover, only microrefugia specific to two herbaceous species were considered. Our findings highlight that shared features exist despite the substantial diversity in habitat characteristics between microrefugia for *O. acetosella* and *A. alpina*. Those common microclimate forcing factors explain a

substantial proportion of the total variance of the degree of decoupling, ranging from 21 to 64%, although we did not estimate different effects for the two species. This indicates that overarching forcing factors contribute significantly to the observed decoupling dynamics, regardless of the species occurring. Those results suggest that microclimatic forcing factors drive the decoupling effects similarly in different ecological contexts, types of ecosystems, or geographic regions. Looking ahead, it would also be particularly insightful to compare plant communities' characteristics and dynamics between microrefugia and their surroundings. We know that plant communities actively respond to microclimatic contrasts at such scales, with species with colder and wetter optimums in microrefugia compared to the immediate vicinity (Finocchiaro et al., 2023), but examining plant traits, and interspecific trait variability could unravel nuanced patterns, shedding light on the factors influencing the diversity and structure of these microclimatic refuges.

While our study includes a control plot and the nearest station to serve as a reference for assessing the decoupling of microrefugia, it is essential to acknowledge the limitation of such study design. The presence of only one paired control site introduces the possibility of site-specific characteristics influencing the observed decoupling dynamics between microrefugia and their surroundings. Ideally, a more robust analysis would involve multiple control sites across various ecological contexts. This approach would provide a more comprehensive understanding of the broader regional climate dynamics in diverse topographic and forest contexts, potentially uncovering a mosaic of diverse microclimates within regional landscape elements that may play a role in shaping different degrees of decoupling.

Identifying and protecting existing microrefugia become imperative components of effective conservation strategies (Hylander et al., 2022). Even though the species studied here may not be under immediate threat, conducting similar investigations to locate microrefugia for prioritized species can be a strategic and proactive approach (García et al., 2020). Efficient detection and protection of these microclimatic refuges are crucial steps toward preserving biodiversity and enhancing the resistance of plant communities in the face of ongoing environmental challenges (Xu et al., 2022). Microrefugia's unique ability to provide stable microclimates can serve as essential components in broader

conservation initiatives and climate change adaptation plans. Recognizing and safeguarding these microclimatic refuges can contribute to the preservation of specific species and the overall ecological resistance of diverse ecosystems.

5. Conclusion

Our primary objective was to rigorously test the definition of microrefugia, conceptualized as sites sheltering species beyond their range amidst unfavorable regional climatic conditions. The sheltering effect relies on specific microclimatic conditions, resulting in a buffering of temperatures and a decoupling effect, crucial for the persistence of populations within these sites in the face of climate change. While existing literature explores the impact of topography and forests on climate, identifying factors favoring disconnected climatic regimes, our article offers a complementary perspective by delving into the current microrefugia's microclimatic characteristics.

In this study, we have explored the unique phenomenon of climatic decoupling within microrefugia—distinctive habitats that exhibit a notable disparity in climatic regimes compared to their surrounding areas. While continued research and monitoring of microrefugia over the long term will be crucial to test the generalization of our results, our observations suggest their pivotal role of microrefugia as potential climatic sanctuaries for plants that maintain outside their range margin, with an inherent capacity to disconnect from prevailing climate trends and extreme events that may occur, such as heatwaves. This highlights their potential to serve as stable refugia, offering advantageous conditions for plant communities (and probably for other taxa) in the face of ongoing climate change. Our investigation has also shed light on factors contributing to the observed short-term decoupling effect, such as the degree of relative elevation, incoming solar radiation, or the percentage of canopy cover. Our study contributes significantly to bridging the gap between broader landscape-scale studies and the specific microclimate dynamics within microrefugia, revealing their potential regarding biodiversity conservation efforts.

Acknowledgments

This work was supported by the Région Provence-Alpes-Côte d'Azur, as part as "Emploi Jeunes Doctorants 2020-2023" grant for the Phd Thesis of Marie Finocchiaro entitled "Conservation de la flore face au réchauffement climatique: caractériser, cartographier et évaluer le rôle des microrefuges en région Sud-PACA", and as part as a project of the AAP 2020 n°02697 "Adaptation au changement climatique pour préserver la biodiversité régionale". This work is also financially and technically supported by the Institut méditerranéen de biodiversité et d'écologie (IMBE, Aix-Marseille University) and the Conservatoire botanique national méditerranéen. We thank the editor and the reviewers whose insightful comments and constructive feedback have significantly enhanced the quality and clarity of this manuscript.

Conflict of interest

The authors declare that they have no conflict of interest.

Bibliography

Aalto, J., Riihimäki, H., Meineri, E., Hylander, K., & Luoto, M. (2017). Revealing topoclimatic heterogeneity using meteorological station data. *International Journal of Climatology*, *37*(S1), 544–556. https://doi.org/10.1002/joc.5020

Aalto, J., Scherrer, D., Lenoir, J., Guisan, A., & Luoto, M. (2018). Biogeophysical controls on soil-atmosphere thermal differences: Implications on warming Arctic ecosystems. *Environmental Research Letters*, *13*(7), 074003. https://doi.org/10.1088/1748-9326/aac83e

Ashcroft, M. B., & Gollan, J. R. (2012). Fine-resolution (25 m) topoclimatic grids of near-surface (5 cm) extreme temperatures and humidities across various habitats in a large (200 × 300 km) and diverse region. *International Journal of Climatology*, *32*(14), 2134–2148. https://doi.org/10.1002/joc.2428

Ashcroft, M. B., & Gollan, J. R. (2013). Moisture, thermal inertia, and the spatial distributions of near-surface soil and air temperatures: Understanding factors that promote microrefugia. *Agricultural and Forest Meteorology*, *176*, 77–89. https://doi.org/10.1016/j.agrformet.2013.03.008

Aurelle, D., Thomas, S., Albert, C., Bally, M., Bondeau, A., Boudouresque, C.-F., Cahill, A. E., Carlotti, F., Chenuil, A., Cramer, W., Davi, H., De Jode, A., Ereskovsky, A., Farnet, A.-M., Fernandez, C., Gauquelin, T., Mirleau, P., Monnet, A.-C., Prévosto, B., … Fady, B. (2022). Biodiversity, climate change, and adaptation in the Mediterranean. *Ecosphere*, *13*(4), e3915. https://doi.org/10.1002/ecs2.3915

Bátori, Z., Gallé, R., Gallé-Szpisjak, N., Császár, P., Nagy, D. D., Lőrinczi, G., Torma, A., Tölgyesi, C., Maák, I. E., Frei, K., Hábenczyus, A. A., & Hornung, E. (2022). Topographic depressions provide potential microrefugia for ground-dwelling arthropods. *Elementa: Science of the Anthropocene*, *10*(1), 00084. https://doi.org/10.1525/elementa.2021.00084

Bátori, Z., Vojtkó, A., Maák, I. E., Lőrinczi, G., Farkas, T., Kántor, N., Tanács, E., Kiss, P. J., Juhász, O., Módra, G., Tölgyesi, C., Erdős, L., Aguilon, D. J., & Keppel, G. (2019). Karst dolines provide diverse microhabitats for different functional groups in multiple phyla. *Scientific Reports*, *9*(1), Article 1. https://doi.org/10.1038/s41598-019-43603-x

Bennie, J., Huntley, B., Wiltshire, A., Hill, M. O., & Baxter, R. (2008). Slope, aspect and climate: Spatially explicit and implicit models of topographic microclimate in chalk grassland. *Ecological Modelling*, *216*(1), 47–59. https://doi.org/10.1016/j.ecolmodel.2008.04.010

Breshears, D. D., Fontaine, J. B., Ruthrof, K. X., Field, J. P., Feng, X., Burger, J. R., Law, D. J., Kala, J., & Hardy, G. E. St. J. (2021). Underappreciated plant vulnerabilities to heat waves. *New Phytologist*, *231*(1), 32–39. https://doi.org/10.1111/nph.17348

Cartereau, M., Leriche, A., Médail, F., & Baumel, A. (2023). Tree biodiversity of warm drylands is likely to decline in a drier world. *Global Change Biology*, *29*(13), 3707–3722. https://doi.org/10.1111/gcb.16722

Cartwright, J. M., Littlefield, C. E., Michalak, J. L., Lawler, J. J., & Dobrowski, S. Z. (2020). Topographic, soil, and climate drivers of drought sensitivity in forests and shrublands of the Pacific Northwest, USA. *Scientific Reports*, *10*(1), Article 1. https://doi.org/10.1038/s41598-020-75273-5

Chapman, S. C., Watkins, N. W., & Stainforth, D. A. (2019). Warming Trends in Summer Heatwaves. *Geophysical Research Letters*, *46*(3), 1634–1640. https://doi.org/10.1029/2018GL081004

Chen, I.-C., Hill, J. K., Ohlemüller, R., Roy, D. B., & Thomas, C. D. (2011). Rapid Range Shifts of Species Associated with High Levels of Climate Warming. *Science*, *333*(6045), 1024–1026. https://doi.org/10.1126/science.1206432

Dan Moore, R., Spittlehouse, D. L., & Story, A. (2005). Riparian Microclimate and Stream Temperature Response to Forest Harvesting: A Review1. *JAWRA Journal of the American Water Resources Association*, *41*(4), 813–834. https://doi.org/10.1111/j.1752-1688.2005.tb03772.x

De Frenne, P., Lenoir, J., Luoto, M., Scheffers, B. R., Zellweger, F., Aalto, J., Ashcroft, M. B., Christiansen, D. M., Decocq, G., De Pauw, K., Govaert, S., Greiser, C., Gril, E., Hampe, A., Jucker, T., Klinges, D. H., Koelemeijer, I. A., Lembrechts, J. J., Marrec, R., … Hylander, K. (2021). Forest microclimates and climate change: Importance, drivers and future research agenda. *Global Change Biology*, *27*(11), 2279–2297. https://doi.org/10.1111/gcb.15569

de Medeiros, C. M., Hernández-Lambraño, R. E., Ribeiro, K. A. F., & Sánchez Agudo, J. Á. (2018). Living on the edge: Do central and marginal populations of plants differ in habitat suitability? *Plant Ecology*, *219*(9), 1029–1043. https://doi.org/10.1007/s11258-018-0855-x

Dobrowski, S. Z. (2011). A climatic basis for microrefugia: The influence of terrain on climate. *Global Change Biology*, *17*(2), 1022–1035. https://doi.org/10.1111/j.1365-2486.2010.02263.x

Drake, J. E., Tjoelker, M. G., Vårhammar, A., Medlyn, B. E., Reich, P. B., Leigh, A., Pfautsch, S., Blackman, C. J., López, R., Aspinwall, M. J., Crous, K. Y., Duursma, R. A., Kumarathunge, D., De Kauwe, M. G., Jiang, M., Nicotra, A. B., Tissue, D. T., Choat, B., Atkin, O. K., & Barton, C. V. M. (2018). Trees tolerate an extreme heatwave via sustained transpirational cooling and increased leaf thermal tolerance. *Global Change Biology*, *24*(6), 2390–2402. https://doi.org/10.1111/gcb.14037

Dusenge, M. E., Duarte, A. G., & Way, D. A. (2019). Plant carbon metabolism and climate change: Elevated CO2 and temperature impacts on photosynthesis, photorespiration and respiration. *New Phytologist*, *221*(1), 32–49. https://doi.org/10.1111/nph.15283

Finocchiaro, M., Médail, F., Saatkamp, A., Diadema, K., Pavon, D., & Meineri, E. (2023). Bridging the gap between microclimate and microrefugia: A bottom-up approach reveals strong climatic and biological offsets. *Global Change Biology*, *29*(4), 1024–1036. https://doi.org/10.1111/gcb.16526

Fischer, E. M., & Schär, C. (2010). Consistent geographical patterns of changes in high-impact European heatwaves. *Nature Geoscience*, *3*(6), Article 6. https://doi.org/10.1038/ngeo866

Frei, K., Vojtkó, A., Farkas, T., Erdős, L., Barta, K., E-Vojtkó, A., Tölgyesi, C., & Bátori, Z. (2023). Topographic depressions can provide climate and resource microrefugia for biodiversity. *iScience*, *26*(11). https://doi.org/10.1016/j.isci.2023.108202

Fu, P., & Rich, P. M. (2002). A geometric solar radiation model with applications in agriculture and forestry. *Computers and Electronics in Agriculture*, *37*(1), 25–35. https://doi.org/10.1016/S0168-1699(02)00115-1

García, M. B., Domingo, D., Pizarro, M., Font, X., Gómez, D., & Ehrlén, J. (2020). Rocky habitats as microclimatic refuges for biodiversity. A close-up thermal approach. *Environmental and Experimental Botany*, *170*, 103886. https://doi.org/10.1016/j.envexpbot.2019.103886

Gentili, R., Baroni, C., Caccianiga, M., Armiraglio, S., Ghiani, A., & Citterio, S. (2015). Potential warm-stage microrefugia for alpine plants: Feedback between geomorphological and biological processes. *Ecological Complexity*, *21*, 87–99. https://doi.org/10.1016/j.ecocom.2014.11.006

Gouveia, C. M., Trigo, R. M., Beguería, S., & Vicente-Serrano, S. M. (2017). Drought impacts on vegetation activity in the Mediterranean region: An assessment using remote sensing data and multi-scale drought indicators. *Global and Planetary Change*, *151*, 15–27. https://doi.org/10.1016/j.gloplacha.2016.06.011

GREC-SUD. (2023). *Bilan annuel 2022*. GREC-SUD. http://www.grec-sud.fr/indicateurs-meteorologiques-2/

Greiser, C., Meineri, E., Luoto, M., Ehrlén, J., & Hylander, K. (2018). Monthly microclimate models in a managed boreal forest landscape. *Agricultural and Forest Meteorology*, *250–251*, 147–158. https://doi.org/10.1016/j.agrformet.2017.12.252

Gril, E., Laslier, M., Gallet-Moron, E., Durrieu, S., Spicher, F., Le Roux, V., Brasseur, B., Haesen, S., Van Meerbeek, K., Decocq, G., Marrec, R., & Lenoir, J. (2023). Using airborne LiDAR to map forest microclimate temperature buffering or amplification. *Remote Sensing of Environment*, *298*, 113820. https://doi.org/10.1016/j.rse.2023.113820

Grossiord, C., Buckley, T. N., Cernusak, L. A., Novick, K. A., Poulter, B., Siegwolf, R. T. W., Sperry, J. S., & McDowell, N. G. (2020). Plant responses to rising vapor pressure deficit. *New Phytologist*, *226*(6), 1550–1566. https://doi.org/10.1111/nph.16485

Hannah, L., Flint, L., Syphard, A. D., Moritz, M. A., Buckley, L. B., & McCullough, I. M. (2014). Fine-grain modeling of species' response to climate change: Holdouts, stepping-stones, and microrefugia. *Trends in Ecology & Evolution*, *29*(7), 390–397. https://doi.org/10.1016/j.tree.2014.04.006

Harrison, S., & Noss, R. (2017). Endemism hotspots are linked to stable climatic refugia. *Annals of Botany*, *119*(2), 207–214. https://doi.org/10.1093/aob/mcw248

Hoffrén, R., Miranda, H., Pizarro, M., Tejero, P., & García, M. B. (2022). Identifying the Factors behind Climate Diversification and Refugial Capacity in Mountain Landscapes: The Key Role of Forests. *Remote Sensing*, *14*(7), Article 7. https://doi.org/10.3390/rs14071708

Hylander, K., Ehrlén, J., Luoto, M., & Meineri, E. (2015). Microrefugia: Not for everyone. *AMBIO*, *44*(1), 60–68. https://doi.org/10.1007/s13280-014-0599-3

Hylander, K., Greiser, C., Christiansen, D. M., & Koelemeijer, I. A. (2022). Climate adaptation of biodiversity conservation in managed forest landscapes. *Conservation Biology*, *36*(3), e13847. https://doi.org/10.1111/cobi.13847

IPCC. (2023). *Climate Change 2022 – Impacts, Adaptation and Vulnerability: Working Group II Contribution to the Sixth Assessment Report of the Intergovernmental Panel on Climate Change* (1st ed.). Cambridge University Press. https://doi.org/10.1017/9781009325844

Jucker, T., Hardwick, S. R., Both, S., Elias, D. M. O., Ewers, R. M., Milodowski, D. T., Swinfield, T., & Coomes, D. A. (2018). Canopy structure and topography jointly constrain the microclimate of human-modified tropical landscapes. *Global Change Biology*, *24*(11), 5243–5258. https://doi.org/10.1111/gcb.14415

Jump, A. S., & Peñuelas, J. (2005). Running to stand still: Adaptation and the response of plants to rapid climate change. *Ecology Letters*, *8*(9), 1010–1020. https://doi.org/10.1111/j.1461-0248.2005.00796.x

Keppel, G., Niel, K. P. V., Wardell-Johnson, G. W., Yates, C. J., Byrne, M., Mucina, L., Schut, A. G. T., Hopper, S. D., & Franklin, S. E. (2012). Refugia: Identifying and understanding safe havens for biodiversity under climate change. *Global Ecology and Biogeography*, *21*(4), 393–404. https://doi.org/10.1111/j.1466-8238.2011.00686.x

Keppel, G., Sarnow, U., Biffin, E., Peters, S., Fitzgerald, D., Boutsalis, E., Waycott, M., & Guerin, G. R. (2023). Population decline in a Pleistocene refugium: Stepwise, drought-related dieback of a South Australian eucalypt. *Science of The Total Environment*, *876*, 162697. https://doi.org/10.1016/j.scitotenv.2023.162697

Kolzenburg, R. (2022). The direct influence of climate change on marginal populations: A review. *Aquatic Sciences*, *84*(2), 1–20. https://doi.org/10.1007/s00027-022-00856-5

Köppen, W. (1900). Versuch einer Klassifikation der Klimate, vorzugsweise nach ihren Beziehungen zur Pflanzenwelt. *Geographische Zeitschrift*, *6*(11), 593–611.

Kuhn, E., & Gégout, J.-C. (2019). Highlighting declines of cold-demanding plant species in lowlands under climate warming. *Ecography*, *42*(1), 36–44. https://doi.org/10.1111/ecog.03469

Lenoir, J., Graae, B. J., Aarrestad, P. A., Alsos, I. G., Armbruster, W. S., Austrheim, G., Bergendorff, C., Birks, H. J. B., Bråthen, K. A., Brunet, J., Bruun, H. H., Dahlberg, C. J., Decocq, G., Diekmann,

M., Dynesius, M., Ejrnæs, R., Grytnes, J.-A., Hylander, K., Klanderud, K., … Svenning, J.-C. (2013). Local temperatures inferred from plant communities suggest strong spatial buffering of climate warming across Northern Europe. *Global Change Biology*, *19*(5), 1470–1481. https://doi.org/10.1111/gcb.12129

Lenoir, J., Hattab, T., & Pierre, G. (2017). Climatic microrefugia under anthropogenic climate change: Implications for species redistribution. *Ecography*, *40*(2), 253–266. https://doi.org/10.1111/ecog.02788

LiDAR HD. (2023). *Descriptif de contenu des nuages de points LiDAR* (Version 1.0) [Computer software].

Lookingbill, T. (2003). Spatial estimation of air temperature differences for landscape-scale studies in montane environments. *Agricultural and Forest Meteorology*, *114*(3–4), 141–151. https://doi.org/10.1016/S0168-1923(02)00196-X

López, R., Ramírez-Valiente, J. A., & Pita, P. (2022). How plants cope with heatwaves in a drier environment. *Flora*, *295*, 152148. https://doi.org/10.1016/j.flora.2022.152148

Lundquist, J. D., Pepin, N., & Rochford, C. (2008). Automated algorithm for mapping regions of cold-air pooling in complex terrain. *Journal of Geophysical Research*, *113*(D22). https://doi.org/10.1029/2008JD009879

Magnago, L. F. S., Rocha, M. F., Meyer, L., Martins, S. V., & Meira-Neto, J. A. A. (2015). Microclimatic conditions at forest edges have significant impacts on vegetation structure in large Atlantic forest fragments. *Biodiversity and Conservation*, *24*(9), 2305–2318. https://doi.org/10.1007/s10531-015-0961-1

Médail, F., & Quézel, P. (1997). Hot-Spots Analysis for Conservation of Plant Biodiversity in the Mediterranean Basin. *Annals of the Missouri Botanical Garden*, *84*(1), 112–127. https://doi.org/10.2307/2399957

MedECC. (2020). *Climate and Environmental Change in the Mediterranean Basin – Current Situation and Risks for the Future. First Mediterranean Assessment Report* (Version 1). Zenodo. https://doi.org/10.5281/ZENODO.7224821

Meehl, G. A., & Tebaldi, C. (2004). More Intense, More Frequent, and Longer Lasting Heat Waves in the 21st Century. *Science*, *305*(5686), 994–997. https://doi.org/10.1126/science.1098704

Meineri, E., Dahlberg, C. J., & Hylander, K. (2015). Using Gaussian Bayesian Networks to disentangle direct and indirect associations between landscape physiography, environmental variables and species distribution. *Ecological Modelling*, *313*, 127–136. https://doi.org/10.1016/j.ecolmodel.2015.06.028

Meineri, E., & Hylander, K. (2017). Fine-grain, large-domain climate models based on climate station and comprehensive topographic information improve microrefugia detection. *Ecography*, *40*(8), 1003–1013. https://doi.org/10.1111/ecog.02494

Meleason, M. A., & Quinn, J. M. (2004). Influence of riparian buffer width on air temperature at Whangapoua Forest, Coromandel Peninsula, New Zealand. *Forest Ecology and Management*, *191*(1), 365–371. https://doi.org/10.1016/j.foreco.2004.01.016

Météo France. (2023). https://meteofrance.com/climat/normales/france/provence-alpes-cote-d-azur

Miralles, D. G., Gentine, P., Seneviratne, S. I., & Teuling, A. J. (2019). Land-atmospheric feedbacks during droughts and heatwaves: State of the science and current challenges: Land feedbacks during droughts and heatwaves. *Annals of the New York Academy of Sciences*, *1436*(1), 19–35. https://doi.org/10.1111/nyas.13912

Moudrý, V., Cord, A. F., Gábor, L., Laurin, G. V., Barták, V., Gdulová, K., Malavasi, M., Rocchini, D., Stereńczak, K., Prošek, J., Klápště, P., & Wild, J. (2022). Vegetation structure derived from airborne laser scanning to assess species distribution and habitat suitability: The way forward. *Diversity and Distributions*, *00*, 1–12. https://doi.org/10.1111/ddi.13644

Mu, M., De Kauwe, M. G., Ukkola, A. M., Pitman, A. J., Guo, W., Hobeichi, S., & Briggs, P. R. (2021). Exploring how groundwater buffers the influence of heatwaves on vegetation function during multi-year droughts. *Earth System Dynamics*, *12*(3), 919–938. https://doi.org/10.5194/esd-12-919-2021

Nadeau, C. P., Giacomazzo, A., & Urban, M. C. (2022). Cool microrefugia accumulate and conserve biodiversity under climate change. *Global Change Biology*, *28*(10), 3222–3235. https://doi.org/10.1111/gcb.16143

Notarnicola, R. F., Nicotra, A. B., Kruuk, L. E. B., & Arnold, P. A. (2021). Tolerance of Warmer Temperatures Does Not Confer Resilience to Heatwaves in an Alpine Herb. *Frontiers in Ecology and Evolution*, *9*. https://www.frontiersin.org/articles/10.3389/fevo.2021.615119

Parducci, L., Jørgensen, T., Tollefsrud, M. M., Elverland, E., Alm, T., Fontana, S. L., Bennett, K. D., Haile, J., Matetovici, I., Suyama, Y., Edwards, M. E., Andersen, K., Rasmussen, M., Boessenkool, S., Coissac, E., Brochmann, C., Taberlet, P., Houmark-Nielsen, M., Larsen, N. K., … Willerslev, E. (2012). Glacial Survival of Boreal Trees in Northern Scandinavia. *Science*, *335*(6072), 1083–1086. https://doi.org/10.1126/science.1216043

Parmesan, C., & Hanley, M. E. (2015). Plants and climate change: Complexities and surprises. *Annals of Botany*, *116*(6), 849–864. https://doi.org/10.1093/aob/mcv169

Pastore, M. A., Classen, A. T., D'Amato, A. W., Foster, J. R., & Adair, E. C. (2022). Cold-air pools as microrefugia for ecosystem functions in the face of climate change. *Ecology*, *n/a*(n/a), e3717. https://doi.org/10.1002/ecy.3717

Pecl, G. T., Araújo, M. B., Bell, J. D., Blanchard, J., Bonebrake, T. C., Chen, I.-C., Clark, T. D., Colwell, R. K., Danielsen, F., Evengård, B., Falconi, L., Ferrier, S., Frusher, S., Garcia, R. A., Griffis, R. B., Hobday, A. J., Janion-Scheepers, C., Jarzyna, M. A., Jennings, S., … Williams, S. E. (2017). Biodiversity redistribution under climate change: Impacts on ecosystems and human well-being. *Science*, *355*(6332). https://doi.org/10.1126/science.aai9214

Perkins, S. E., & Alexander, L. V. (2013). On the Measurement of Heat Waves. *Journal of Climate*, *26*(13), 4500–4517. https://doi.org/10.1175/JCLI-D-12-00383.1

Pinheiro, J., & Bates, D. (2023). *nlme: Linear and Nonlinear Mixed Effects Models* (R package version 3.1-164) [Computer software]. R Core Team. https://cran.r-project.org/web/packages/nlme/nlme.pdf

Rameau, J.-C., Mansion, D., & Dumé, G. (1989). *Flore forestière française: Guide écologique illustré*. Forêt privée française.

Ramos, R. F., Franco, A. M. A., Gilroy, J. J., & Silva, J. P. (2023). Combining bird tracking data with high-resolution thermal mapping to identify microclimate refugia. *Scientific Reports*, *13*, 4726. https://doi.org/10.1038/s41598-023-31746-x

Rita, A., Bonanomi, G., Allevato, E., Borghetti, M., Cesarano, G., Mogavero, V., Rossi, S., Saulino, L., Zotti, M., & Saracino, A. (2021). Topography modulates near-ground microclimate in the Mediterranean Fagus sylvatica treeline. *Scientific Reports*, *11*(1), 8122. https://doi.org/10.1038/s41598-021-87661-6

Roussel, J.-R., Auty, D., Coops, N. C., Tompalski, P., Goodbody, T. R. H., Meador, A. S., Bourdon, J.-F., de Boissieu, F., & Achim, A. (2020). lidR: An R package for analysis of Airborne Laser Scanning (ALS) data. *Remote Sensing of Environment*, *251*, 112061. https://doi.org/10.1016/j.rse.2020.112061

Rull, V. (2009). Microrefugia. *Journal of Biogeography*, *36*(3), 481–484. https://doi.org/10.1111/j.1365-2699.2008.02023.x

Rull, V. (2010). On microrefugia and cryptic refugia. *Journal of Biogeography*, *37*(8), 1623–1625. https://doi.org/10.1111/j.1365-2699.2010.02340.x

Russell, V. L. (2021). *emmeans: Estimated Marginal Means, aka Least-Squares Means* (R package version 1.7.0) [Computer software]. https://CRAN.R-project.org/package=emmeans

Sanginés de Cárcer, P., Vitasse, Y., Peñuelas, J., Jassey, V. E. J., Buttler, A., & Signarbieux, C. (2018). Vapor–pressure deficit and extreme climatic variables limit tree growth. *Global Change Biology*, *24*(3), 1108–1122. https://doi.org/10.1111/gcb.13973

Scafaro, A. P., Fan, Y., Posch, B. C., Garcia, A., Coast, O., & Atkin, O. K. (2021). Responses of leaf respiration to heatwaves. *Plant, Cell & Environment*, *44*(7), 2090–2101. https://doi.org/10.1111/pce.14018

Scherrer, D., & Körner, C. (2011). Topographically controlled thermal-habitat differentiation buffers alpine plant diversity against climate warming. *Journal of Biogeography*, *38*(2), 406–416. https://doi.org/10.1111/j.1365-2699.2010.02407.x

Słowińska, S., Słowiński, M., Marcisz, K., & Lamentowicz, M. (2022). Long-term microclimate study of a peatland in Central Europe to understand microrefugia. *International Journal of Biometeorology*. https://doi.org/10.1007/s00484-022-02240-2

Sorel, M., Soubeyroux, J.-M., Drouin, A., Jourdain, S., Kerdoncuff, M., Cassaigne, B., Théron, M.-H., Josse, P., & Lacanal, C. (2022). Normales climatiques 1991-2020. *La Météorologie*, *2022*(119), 73–79. https://doi.org/10.37053/lameteorologie-2022-0086

Soubeyroux, J.-M., Ouzeau, G., Schneider, M., Cabanes, O., & Kounkou-Arnaud, R. (2016). Les vagues de chaleur en France: Analyse de l'été 2015 et évolutions attendues en climat futur. *La Météorologie*, *8*(94), 45. https://doi.org/10.4267/2042/60704

Thom, D., Ammer, C., Annighöfer, P., Aszalós, R., Dittrich, S., Hagge, J., Keeton, W. S., Kovacs, B., Krautkrämer, O., Müller, J., von Oheimb, G., & Seidl, R. (2023). Regeneration in European beech forests after drought: The effects of microclimate, deadwood and browsing. *European Journal of Forest Research*, *142*(2), 259–273. https://doi.org/10.1007/s10342-022-01520-1

Thorne, J. H., Boynton, R. M., Hollander, A. D., Flint, L. E., Flint, A. L., & Urban, D. (2023). The Contribution of Microrefugia to Landscape Thermal Inertia for Climate-Adaptive Conservation Strategies. *Earth's Future*, *11*(6), e2022EF003338. https://doi.org/10.1029/2022EF003338

Vignal, M. (2020). *L'impact du changement global sur la flore du Sud-Est de la France: Modélisation multiscalaire de la répartition de 25 espèces à l'horizon 2100 par la dynamique de population*. Université Côte d'Azur.

Wang, P., Li, D., Liao, W., Rigden, A., & Wang, W. (2019). Contrasting Evaporative Responses of Ecosystems to Heatwaves Traced to the Opposing Roles of Vapor Pressure Deficit and Surface Resistance. *Water Resources Research*, *55*(6), 4550–4563. https://doi.org/10.1029/2019WR024771

Whalen, M. A., Starko, S., Lindstrom, S. C., & Martone, P. T. (2023). Heatwave restructures marine intertidal communities across a stress gradient. *Ecology*, *104*(5), e4027. https://doi.org/10.1002/ecy.4027

Williamson, J., Slade, E. M., Luke, S. H., Swinfield, T., Chung, A. Y. C., Coomes, D. A., Heroin, H., Jucker, T., Lewis, O. T., Vairappan, C. S., Rossiter, S. J., & Struebig, M. J. (2021). Riparian buffers act as microclimatic refugia in oil palm landscapes. *Journal of Applied Ecology*, *58*(2), 431–442. https://doi.org/10.1111/1365-2664.13784

Wolf, C., Bell, D. M., Kim, H., Nelson, M. P., Schulze, M., & Betts, M. G. (2021). Temporal consistency of undercanopy thermal refugia in old-growth forest. *Agricultural and Forest Meteorology*, *307*, 108520. https://doi.org/10.1016/j.agrformet.2021.108520

Xu, X., Huang, A., Belle, E., De Frenne, P., & Jia, G. (2022). Protected areas provide thermal buffer against climate change. *Science Advances*, *8*(44), eabo0119. https://doi.org/10.1126/sciadv.abo0119

Yuan, W., Zheng, Y., Piao, S., Ciais, P., Lombardozzi, D., Wang, Y., Ryu, Y., Chen, G., Dong, W., Hu, Z., Jain, A. K., Jiang, C., Kato, E., Li, S., Lienert, S., Liu, S., Nabel, J. E. M. S., Qin, Z., Quine, T., … Yang, S. (2019). Increased atmospheric vapor pressure deficit reduces global vegetation growth. *Science Advances*, *5*(8), eaax1396. https://doi.org/10.1126/sciadv.aax1396

Zellweger, F., De Frenne, P., Lenoir, J., Rocchini, D., & Coomes, D. (2019). Advances in Microclimate Ecology Arising from Remote Sensing. *Trends in Ecology & Evolution*, *34*(4), 327–341. https://doi.org/10.1016/j.tree.2018.12.012

Zellweger, F., De Frenne, P., Lenoir, J., Vangansbeke, P., Verheyen, K., Bernhardt-Römermann, M., Baeten, L., Hédl, R., Berki, I., Brunet, J., Van Calster, H., Chudomelová, M., Decocq, G., Dirnböck, T., Durak, T., Heinken, T., Jaroszewicz, B., Kopecký, M., Máliš, F., … Coomes, D. (2020). Forest microclimate dynamics drive plant responses to warming. *Science*, *368*(6492), 772–775. https://doi.org/10.1126/science.aba6880

Zhang, S., Landuyt, D., Verheyen, K., & De Frenne, P. (2022). Tree species mixing can amplify microclimate offsets in young forest plantations. *Journal of Applied Ecology*, *59*(6), 1428–1439. https://doi.org/10.1111/1365-2664.14158

Figure captions

Figure 1: Putative microrefugia of *Arabis alpina* (orange dots) and *Oxalis acetosella* (green dots) in the study region of South-eastern France (PACA region). Red triangles are indicative of the nearest weather stations of each site. The red line delineates the national boundary between Italy and France, and the white lines delineate the boundaries of the administrative regions of France. Credits for map base: Esri, HERE, DeLorme, increment P Corp., NPS, NRCan, Ordonance Survey, © OpenStreetMap contributors, USGS, NGA, NASA, CGIAR, N Robinson, NCEAS, NLS, OS, NMA, Geodatastyrelsen, Rijkswaterstaat, GSA, Geolan, FEMA, Intermap and the GIS user community.

Figure 2: Conceptual figure, illustrating the detection method of a heatwave event (colored in light-red) for each weather station, based on its daily temperatures (black line). The 99.5^{th} percentile (Spic in dashed red) and the 97.5^{th} percentile (S in dashed green) are computed thanks to the 30-years historical data of the 3 nearest weather stations. A heatwave occurs if the threshold Spic is reached at least once. Start and end date are defined when temperature respectively passes upon and down the threshold S after at least 3 days. Green arrows refer to the non-heatwave period of 10 days period before and 10 days after each heatwave that was inputted in the analysis of heatwave impact on the degree of decoupling.

Figure 3: Patterns of microclimatic decoupling. **(a)** Temperatures dynamics at a regional scale (referred to as "Macroclimate", in orange), along with the temperature trends observed at two specific sites. Site A (in red) follows the regional temperature patterns, while Site B (in blue) exhibits independent temperature fluctuations that deviate from the macroclimate. **(b)** The linear relationship between microclimatic conditions in Site A and the macroclimate is characterized by a slope equal to 1 (in red), indicating a perfect coupling between the two variables. On the other hand, the linear relationship between the microclimate observed in Site B and the macroclimate displays a slope of 0 (in blue), representing the site's capacity for perfect decoupling from the regional climatic conditions. Here, the p-value associated with the regression slope test if the latter is significantly different from 0, i.e. test for significant deviation from perfect decoupling. **(c)** The linear relationship between the temperature differences between the microclimate measured in Site A and the macroclimate against

the macroclimate is characterized by a slope equal to 0 (in red), indicating a perfect correlation of temperatures between Site A and the macroclimate. The linear relationship between temperature differences between the macroclimate and Site B microclimate is characterized by a slope equal to -1 (in blue), representing a total decorrelation between temperatures in Site B and the macroclimate. Here, p-values associated with the regression slope test if the slope is significantly different from 0, i.e. test for significant deviation from the perfect coupling. These figures are inspired by the works of Dobrowski (2011) and De Frenne et al. (2021).

Figure 4: Regression slopes extracted from linear mixed models of the linear relationships of the differences of temperatures in microrefugia and control plots against control plots temperatures, and the differences of temperatures between the nearest weather station and microrefugia against nearest weather stations temperatures, for daily mean, maximum and minimum temperatures. It is important to note that we deliberately omit consideration of the intercept component to focus exclusively on plotting the slope estimates, thereby offering a clearer depiction of the relationships under examination (the figure including the intercept values can be found in **Annex 2**).

Figure 5: Estimated degree of the slope of the linear relationship describing how the difference in temperature between microrefugia and nearest weather station **(a)** or surrounding plots **(b)** respond to temperature variations outside and during heatwave events (respectively "non-HW" and "HW" in green and red). Slope values are extracted for the mean (TMean), maximum (TMax), and minimum (TMin) temperatures. P-values are extracted from the models and Tukey pairwise post-hoc comparison tests. Error bars refer to the standard deviation of each estimate in the models, with their associated p-values at the bottom of each bar (with *** = p<.0001 and * = p<0.05). P-values under each black line refer to the significant difference in the degree of decoupling between non-heatwave and heatwave periods.

Figure 6: Estimated offsets of VPD between microrefugia, control plots, and nearest weather stations, extracted from Tukey posthoc tests carried out on linear mixed models of **(a)** mean VPD, **(b)** maximum VPD and **(c)** minimum VPD as a function of type of plot (microrefugia, control plots or

nearest weather station), and heatwave events (HW = heatwave event; non-HW = non-heatwave event) on a reduced dataset around heatwave' events.

Figure 7: Estimated degree of the slope of the linear relationship describing how the difference in VPD between microrefugia and nearest weather station **(a)** or surrounding plots **(b)** respond to VPD variations outside and during heatwave events (respectively "non-HW" and "HW" in green and red). Slope values are extracted for the mean (VPDMean), maximum (VPDMax), and minimum (VPDMin) VPD. P-values are extracted from the models and Tukey pairwise post-hoc comparison tests. Error bars refer to the standard deviation of each estimate in the models, with their associated p-values at the bottom of each bar (with *** = p<.0001 and * = p<0.05). P-values under each black line refer to the significant difference in the degree of decoupling between non-heatwave and heatwave periods.

Declaration of interests

☐The authors declare that they have no known competing financial interests or personal relationships that could have appeared to influence the work reported in this paper.

☒The authors declare the following financial interests/personal relationships which may be considered as potential competing interests:

Marie Finocchiaro reports financial support was provided by Région Provence-Alpes-Côte d'Azur. Eric Meineri reports financial support was provided by Région Provence-Alpes-Côte d'Azur. Marie Finocchiaro reports financial support was provided by Conservatoire Botanique National Méditerranéen. If there are other authors, they declare that they have no known competing financial interests or personal relationships that could have appeared to influence the work reported in this paper.

Author Contributions Statement

Marie Finocchiaro: Conceptualization ; Data curation ; Formal analysis ; Investigation ; Methodology ; Visualization ; Writing – original draft ; Writing – review & editing
Frédéric Médail: Conceptualization ; Funding acquisition ; Investigation ;Project administration ; Supervision ; Validation ; Writing – review & editing
Arne Saatkamp: Writing – review & editing
Katia Diadema: Writing – review & editing
Daniel Pavon: Writing – review & editing
Lenka Brousset: Writing – review & editing
Eric Meineri : Conceptualization ; Funding acquisition ; Investigation ; Methodology ; Project administration ; Supervision ; Validation ; Writing – review & editing

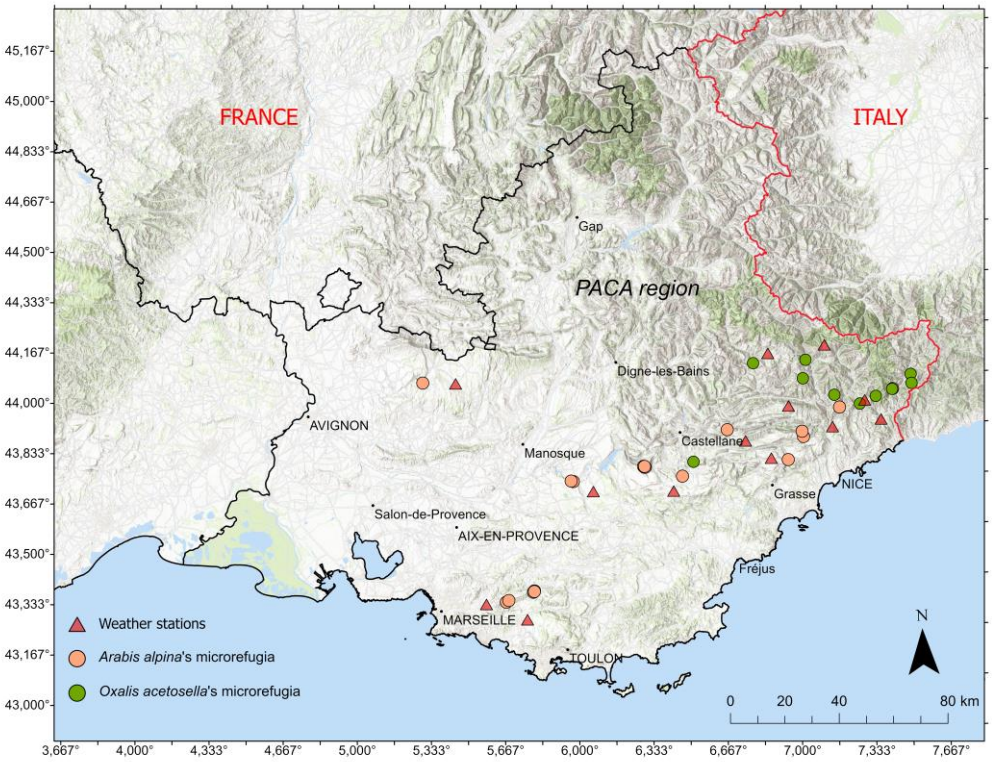

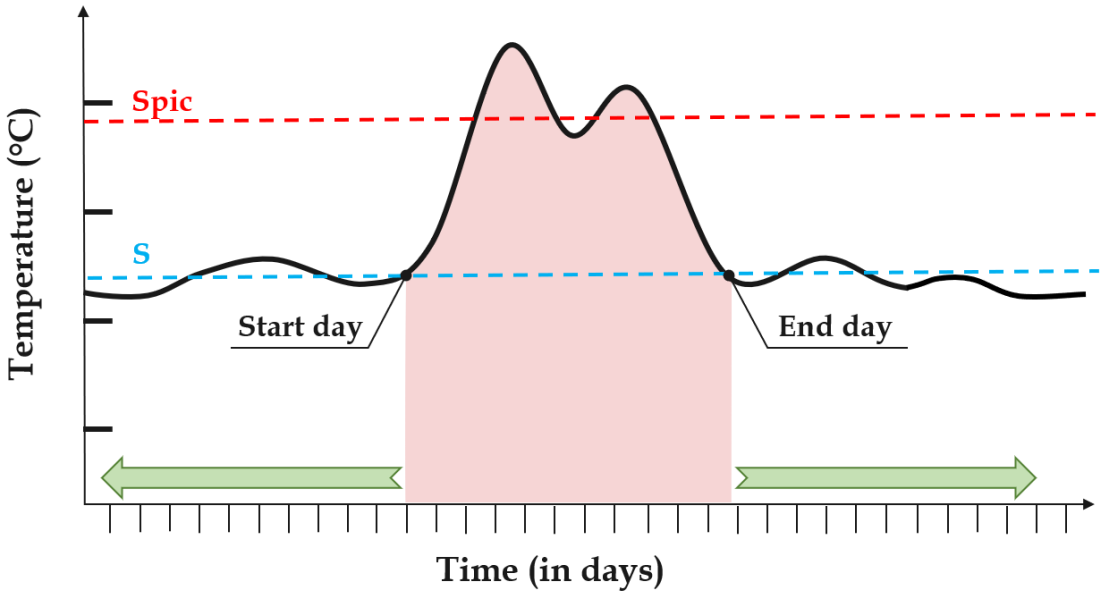

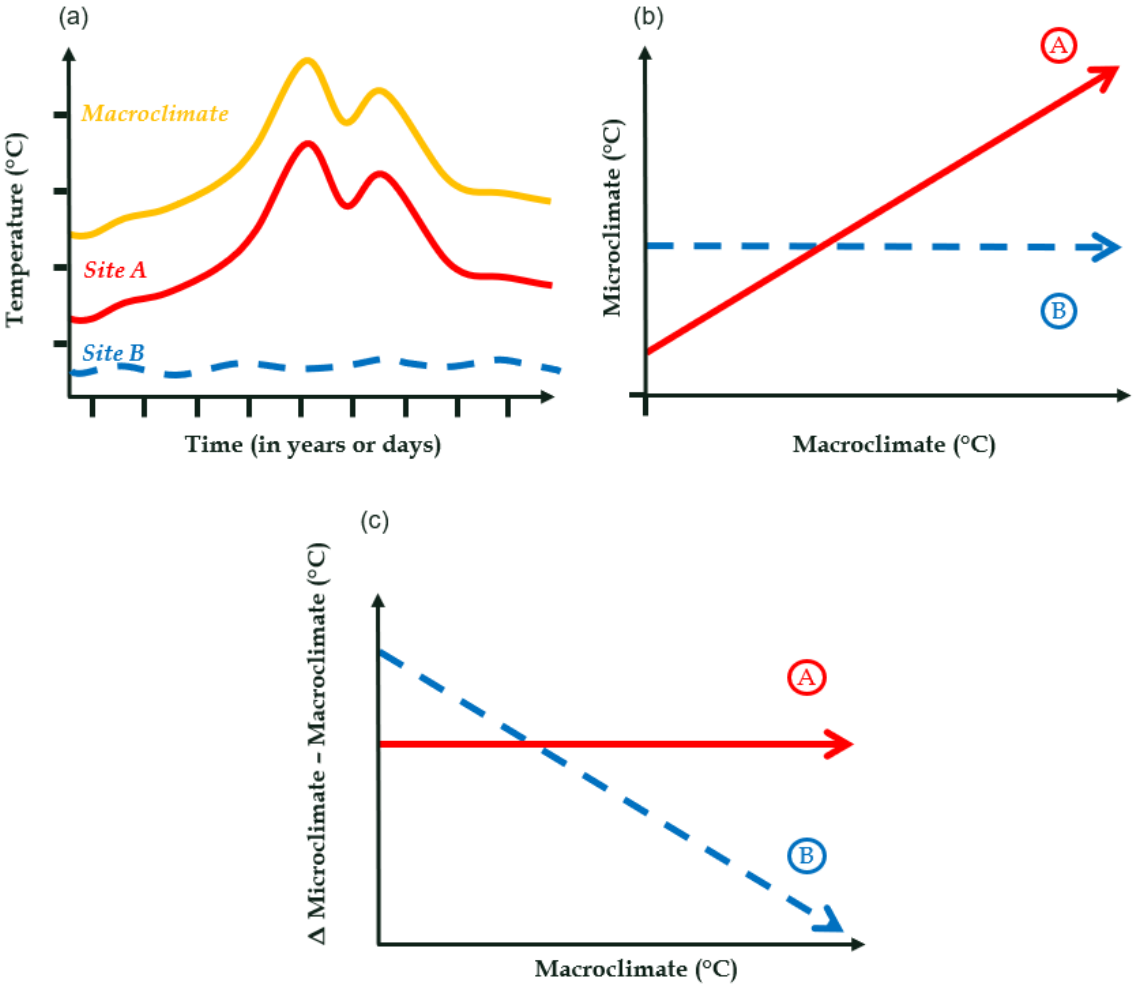
(a)
Macroclimate
Site A
Site B
Temperature (°C)
Time (in years or days)
(b)
A
B
Microclimate (°C)
Macroclimate (°C)
(c)
A
B
Δ Microclimate – Macroclimate (°C)
Macroclimate (°C)

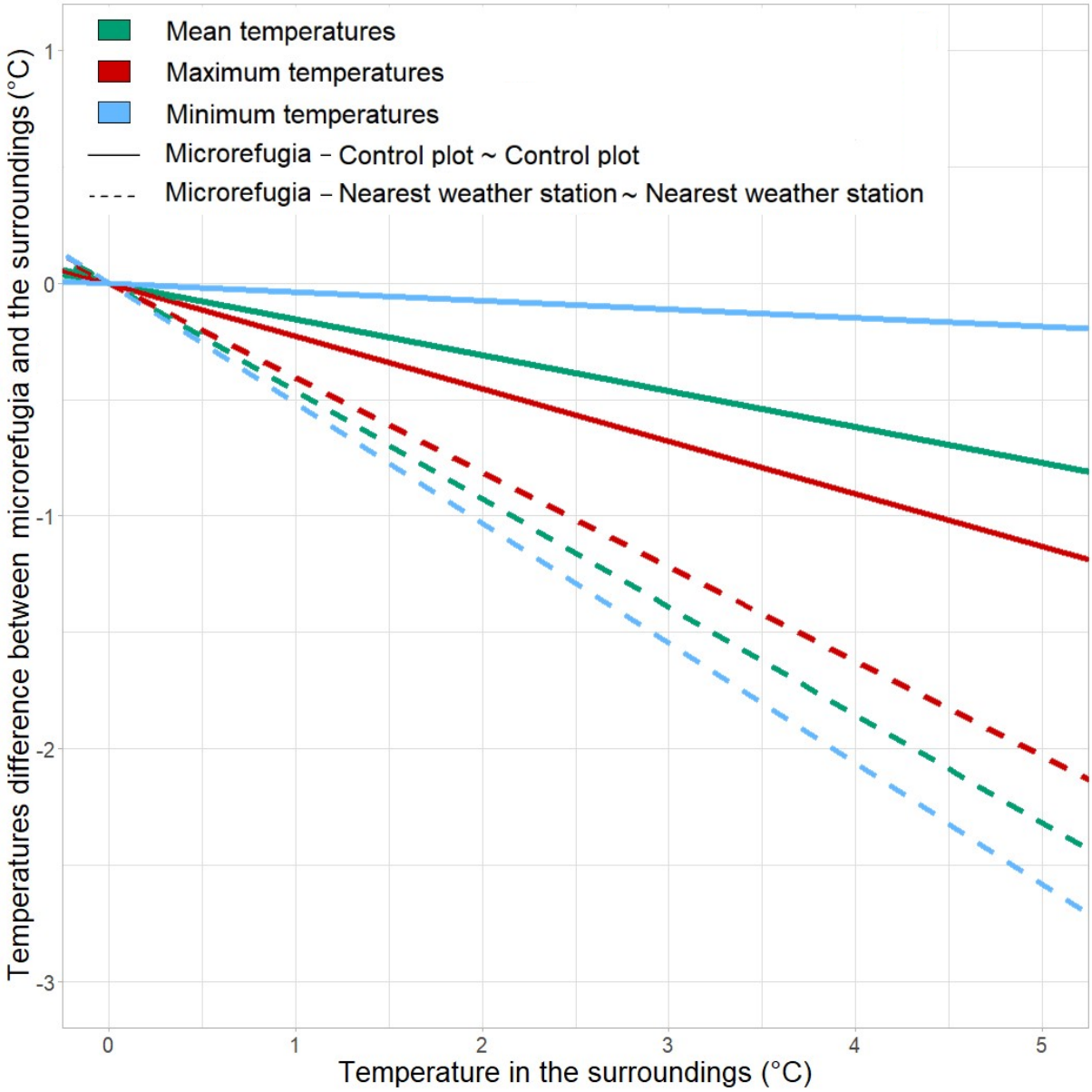
Mean temperatures
Maximum temperatures
Minimum temperatures
Microrefugia – Control plot ~ Control plot
Microrefugia – Nearest weather station ~ Nearest weather station
Temperatures difference between microrefugia and the surroundings (°C)
1
0
-1
-2
-3
0
1
2
3
4
5
Temperature in the surroundings (°C)

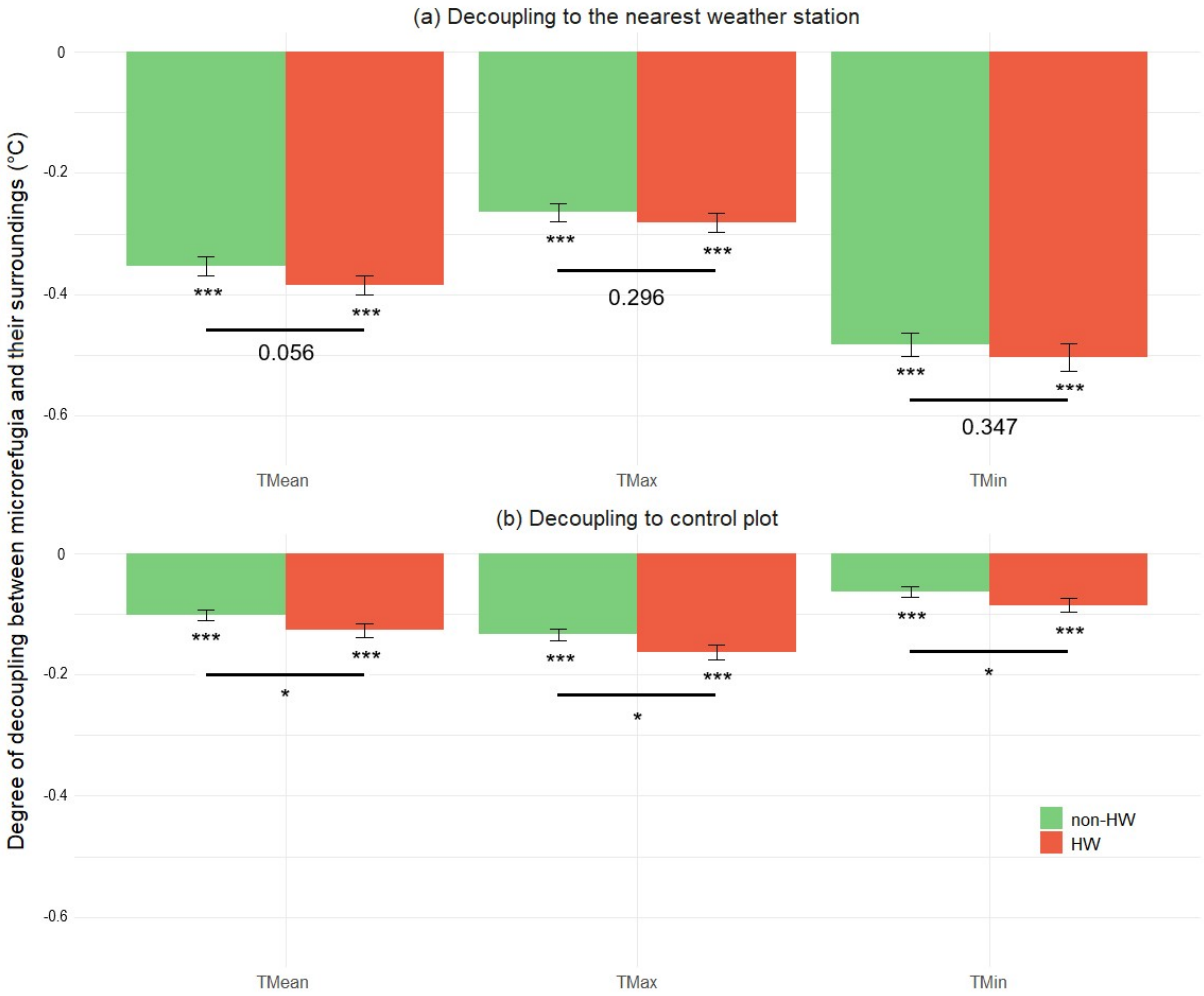
(a) Decoupling to the nearest weather station
Degree of decoupling between microrefugia and their surroundings (°C)
0
-0.2
-0.4
-0.6
***
***
0.056
***
***
0.296
***
***
0.347
TMean
TMax
TMin
(b) Decoupling to control plot
0
-0.2
-0.4
-0.6
***
***
*
***
***
*
***
***
*
non-HW
HW
TMean
TMax
TMin

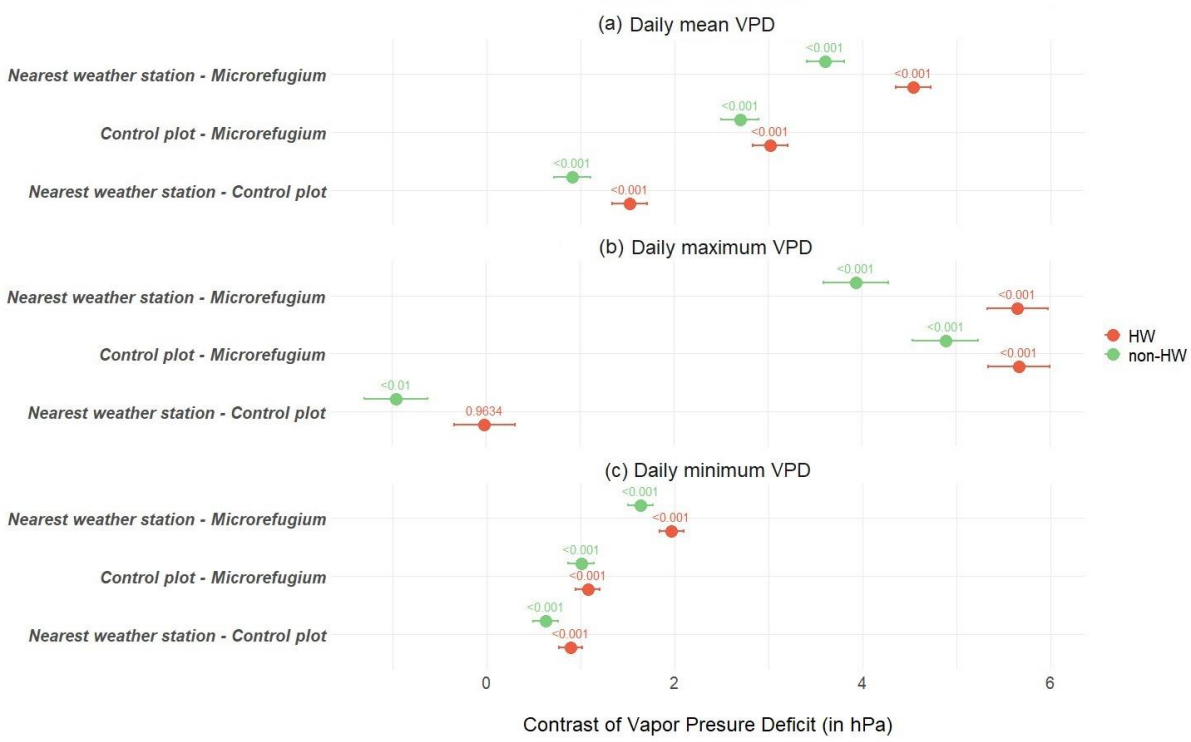

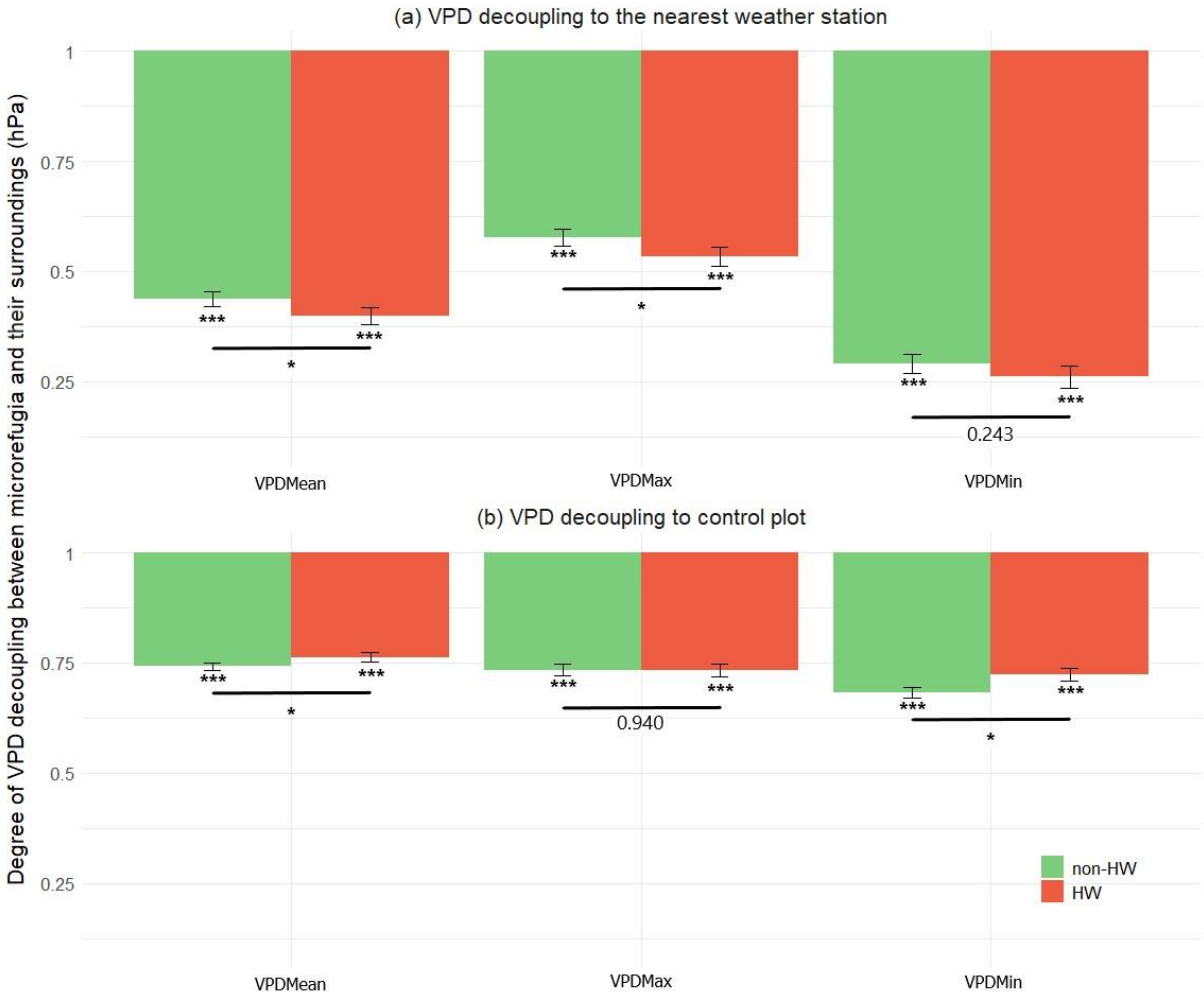
(a) VPD decoupling to the nearest weather station
Degree of VPD decoupling between microrefugia and their surroundings (hPa)
1
0.75
0.5
0.25
***
***
*
***
***
*
***
***
0.243
VPDMean
VPDMax
VPDMin
(b) VPD decoupling to control plot
1
0.75
0.5
0.25
***
***
*
***
***
0.940
***
***
*
non-HW
HW
VPDMean
VPDMax
VPDMin

Table 1: Summary of regression models of differences in mean (ΔTMean), maximum Δ (TMax), and minimum (ΔTMin) temperatures between microrefugia and nearest weather stations against temperatures in the nearest weather stations (upper part of the table), between microrefugia and control plots against temperatures in control plots (middle part of the table), and between control plots and nearest weather stations against temperatures in the nearest weather stations (lower part of the table). The models present regression slope estimates and corresponding p-values (p).

	ΔT_{Mean}		**ΔT_{Max}**		**ΔT_{Min}**	
Predictors	Estimates	*p*	Estimates	*P*	Estimates	*p*
(Intercept)	5.530	<0.001	6.126	<0.001	4.026	<0.001
Degree of decoupling of microrefugia to the nearest weather stations (regression slope)	**-0.464**	<0.001	**-0.406**	<0.001	**-0.516**	<0.001
(Intercept)	1.096	<0.001	2.507	<0.001	-0.098	0.805
Degree of decoupling of microrefugia to the control plots (regression slope)	**-0.154**	<0.001	**-0.226**	<0.001	**-0.037**	<0.001
(Intercept)	4.251	<0.001	2.913	0.002	3.309	<0.001
Degree of decoupling of the control plots to the nearest weather stations (regression slope)	**-0.302**	<0.001	**-0.133**	<0.001	**-0.399**	<0.001

Decoupling between microrefugia and weather stations	TMean		TMax		TMin	
	Estimate	p-value	Estimate	p-value	Estimate	p-value
(Intercept)	-0.435	<.001	-0.426	<.001	_	_
Δ Distance to nearest stream section	_	_	_	_	_	_
Δ Relative elevation (500m radius)	-0.114	0.002	_	_	_	_
Δ Incoming solar radiation	_	_	-0.073	0.007	_	_
Percentage of Canopy cover in microrefugia	_	_	_	_	_	_
Standard deviation of tree height in microrefugia	_	_	_	_	_	_
Mean Vegetation Height in microrefugia	_	_	-0.113	<.001	_	_
R^2 of the model	0.342		0.641		_	

Decoupling between microrefugia and control plots	TMean		TMax		TMin	
	Estimate	p-value	Estimate	p-value	Estimate	p-value
(Intercept)	-0.116	<.001	-0.207	<.001	-0.119	<.001
Δ Distance to nearest stream section	_	_	_	_	-0.052	0.009
Δ Relative elevation (500m radius)	_	_	_	_	_	_
Δ Incoming solar radiation	_	_	-0.106	0.018	_	_
Δ Percentage of Canopy cover	_	_	_	_	_	_
Δ Standard deviation of tree height	0.061	0.015	_	_	_	_
Δ Mean Vegetation Height	_	_	_	_	_	_
R^2 of the model	0.208		0.251		0.281	

Table 2: Results of linear mixed models performed on the degree of decoupling of each site, extracted form GLS, against (i) the deltas of topographic features between the nearest weather station and microrefugia, and forest-related features in microrefugia (upper part of the table) (ii) the deltas of topographic and forest-related features between the control plots and microrefugia (bottom part of the

table). Underscores refer to variables not selected during the stepwise process due to their lack of significance.

Graphical abstract

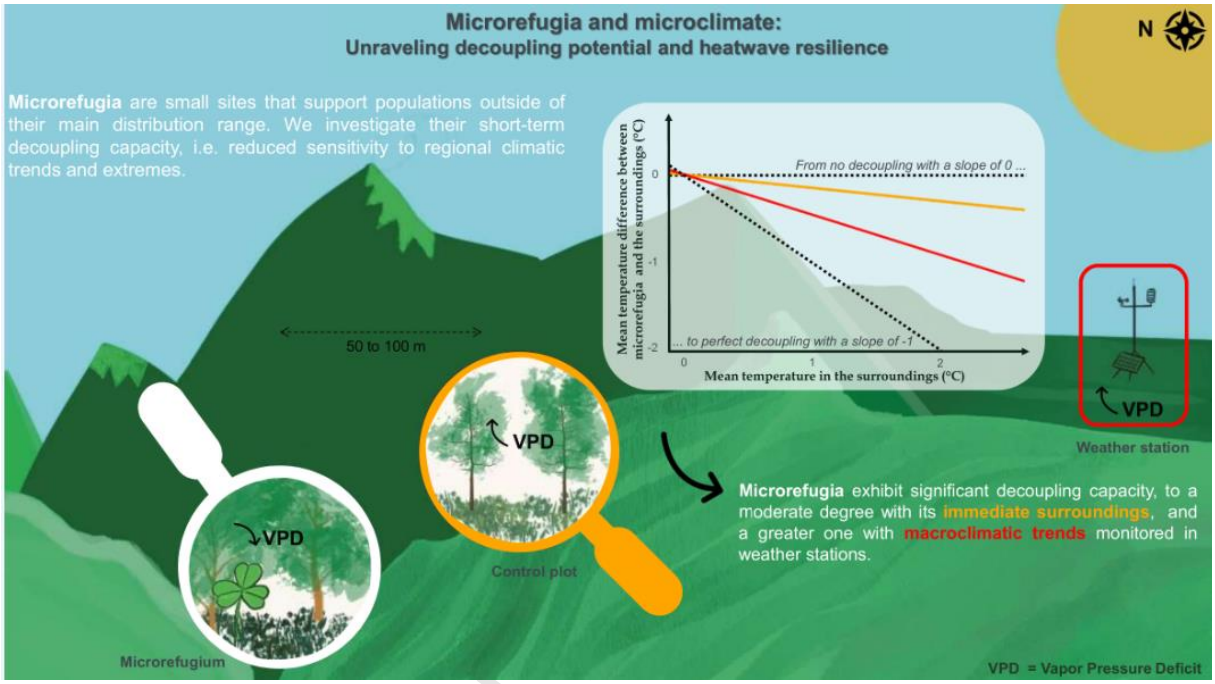

Highlights

- We demonstrate a decoupling between microrefugia's microclimate and macroclimate
- Landscape features partly explain this short-term decoupling
- Microrefugia exhibit lower Vapor Pressure Deficit, particularly during heatwaves
- Microrefugia with sustained decoupling may act as stable enclaves for species

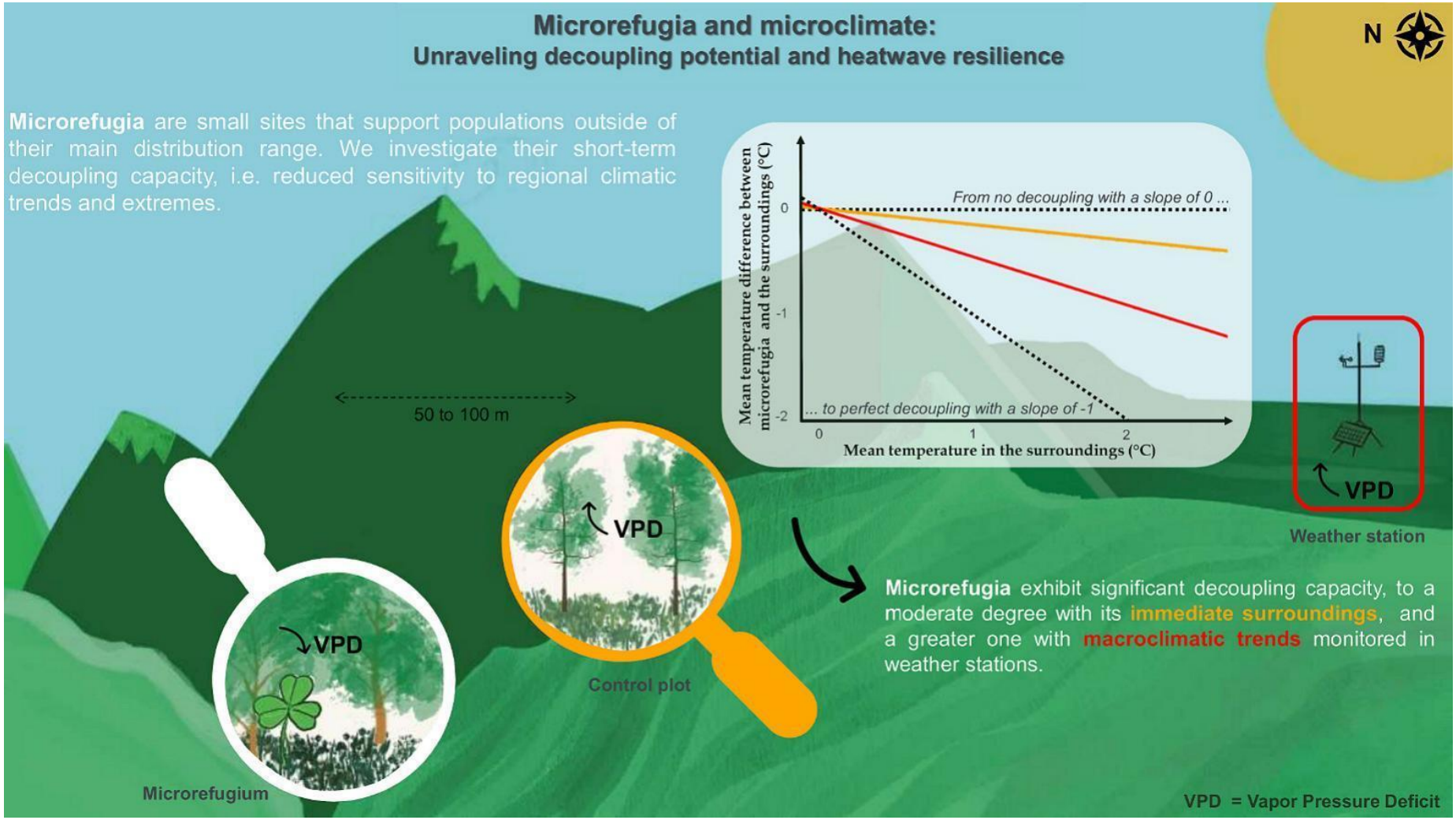

Graphics Abstract

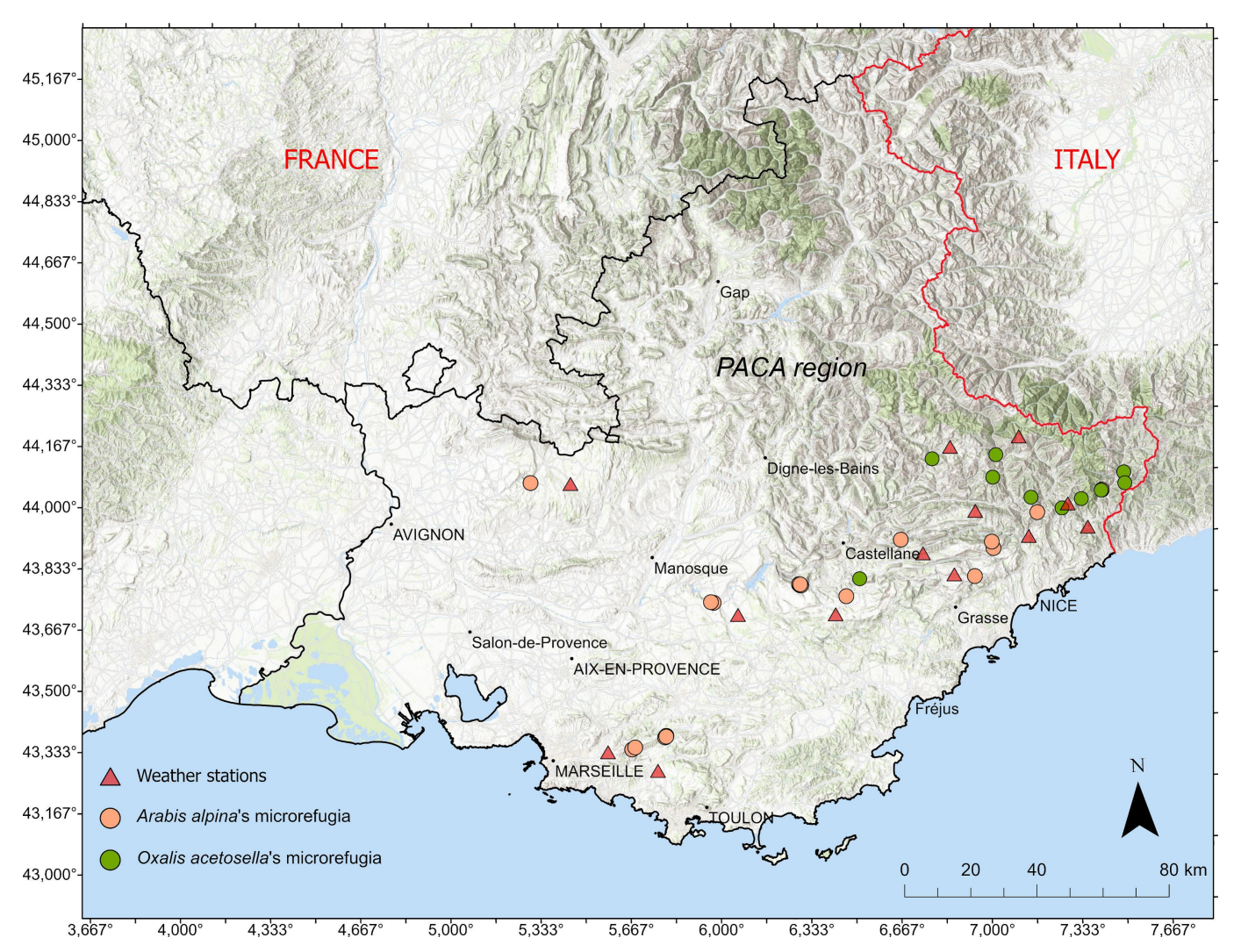
FRANCE
ITALY
PACA region
Gap
Digne-les-Bains
AVIGNON
Manosque
Castellane
Grasse
NICE
Salon-de-Provence
AIX-EN-PROVENCE
Fréjus
MARSEILLE
TOULON
Weather stations
Arabis alpina's microrefugia
Oxalis acetosella's microrefugia
N
0 20 40 80 km
45,167°
45,000°
44,833°
44,667°
44,500°
44,333°
44,167°
44,000°
43,833°
43,667°
43,500°
43,333°
43,167°
43,000°
3,667°
4,000°
4,333°
4,667°
5,000°
5,333°
5,667°
6,000°
6,333°
6,667°
7,000°
7,333°
7,667°

Figure 1

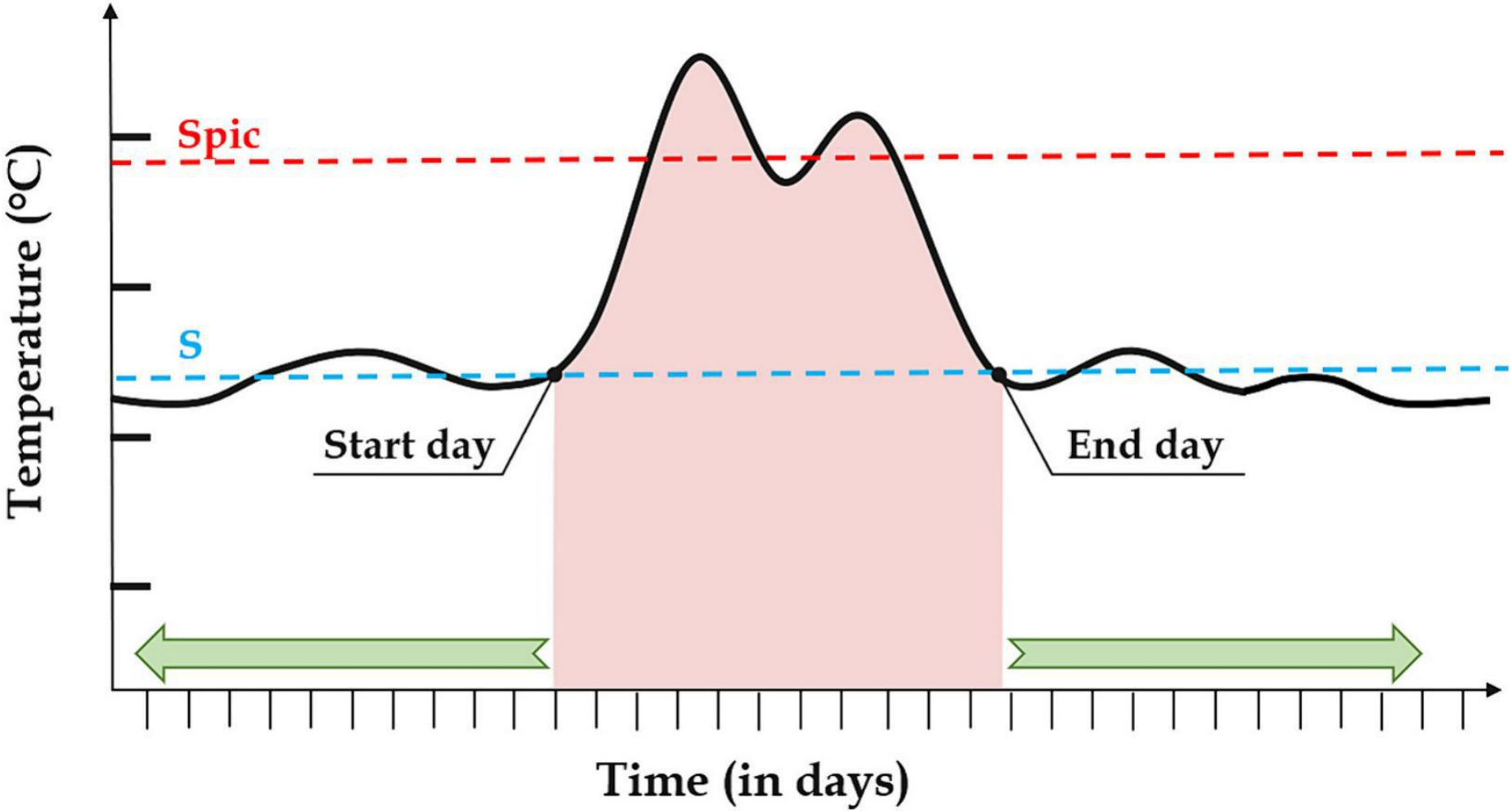

Figure 2

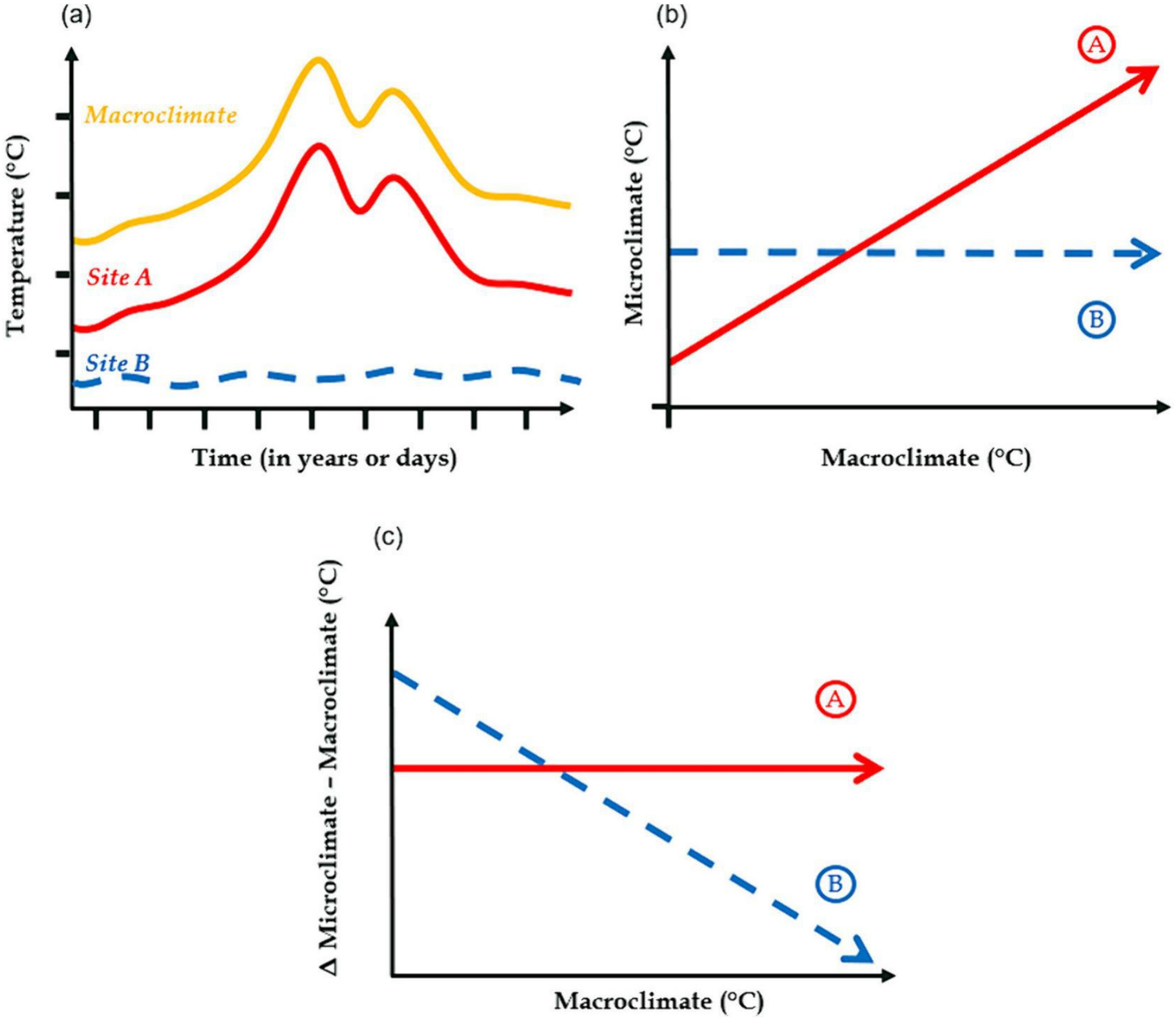
(a)
Macroclimate
Site A
Site B
Temperature (°C)
Time (in years or days)
(b)
A
B
Microclimate (°C)
Macroclimate (°C)
(c)
A
B
Δ Microclimate – Macroclimate (°C)
Macroclimate (°C)

Figure 3

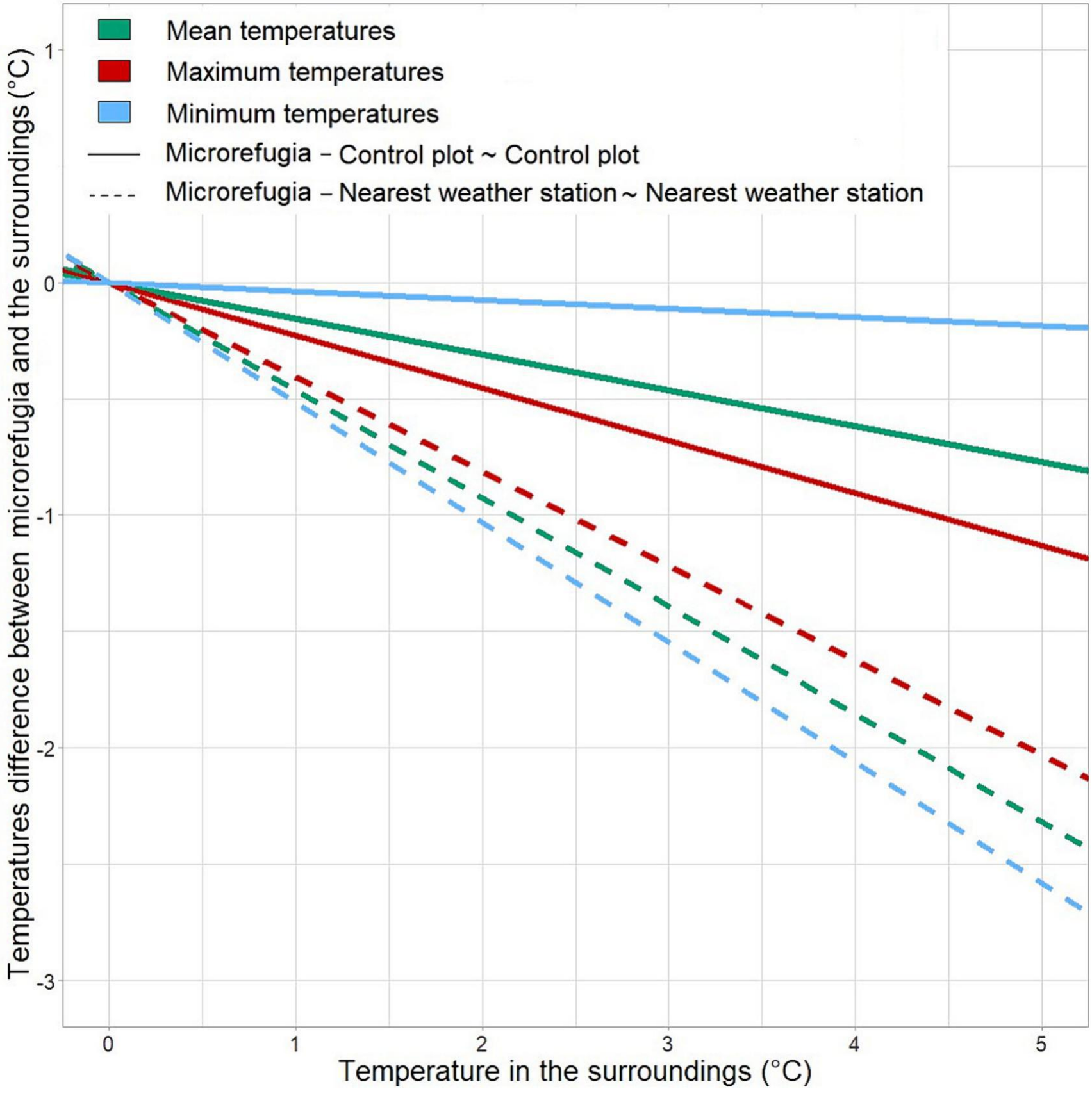
Mean temperatures
Maximum temperatures
Minimum temperatures
Microrefugia – Control plot ~ Control plot
Microrefugia – Nearest weather station ~ Nearest weather station
Temperatures difference between microrefugia and the surroundings (°C)
1
0
-1
-2
-3
0
1
2
3
4
5
Temperature in the surroundings (°C)

Figure 4

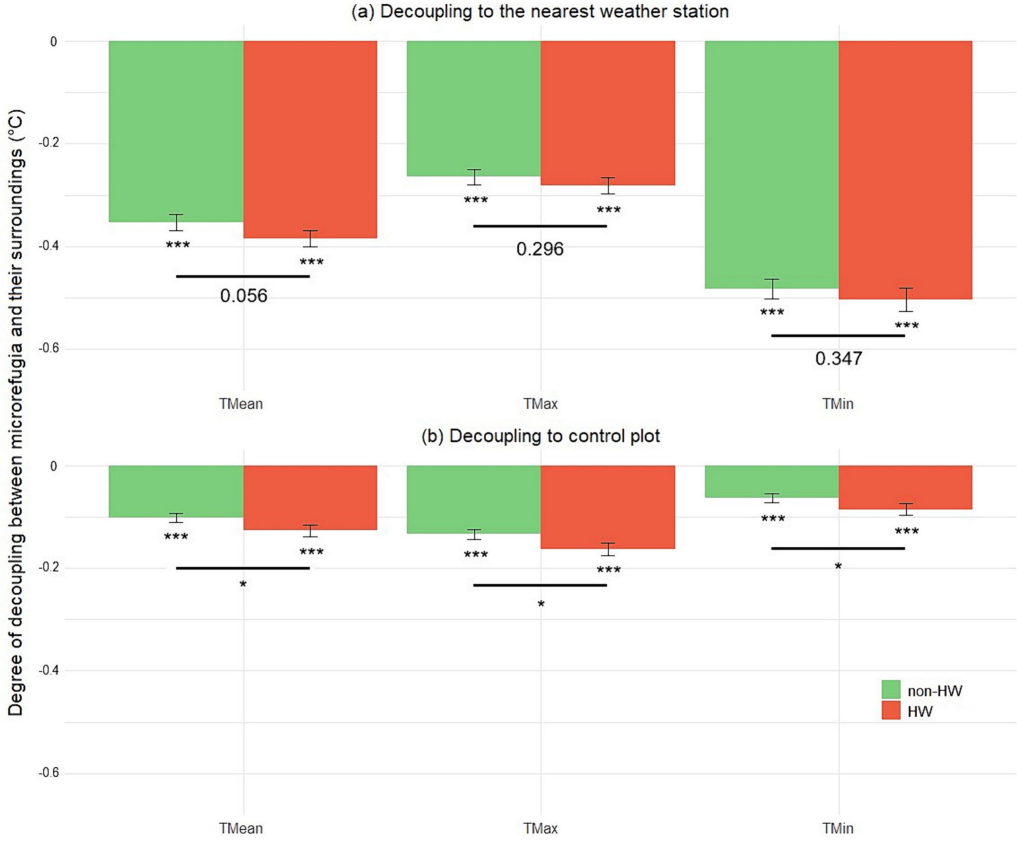
(a) Decoupling to the nearest weather station
Degree of decoupling between microrefugia and their surroundings (°C)
0
-0.2
-0.4
-0.6
***
***
0.056
***
***
0.296
***
***
0.347
TMean
TMax
TMin
(b) Decoupling to control plot
0
-0.2
-0.4
-0.6
***
***
*
***
***
*
***
***
*
TMean
TMax
TMin
non-HW
HW

Figure 5

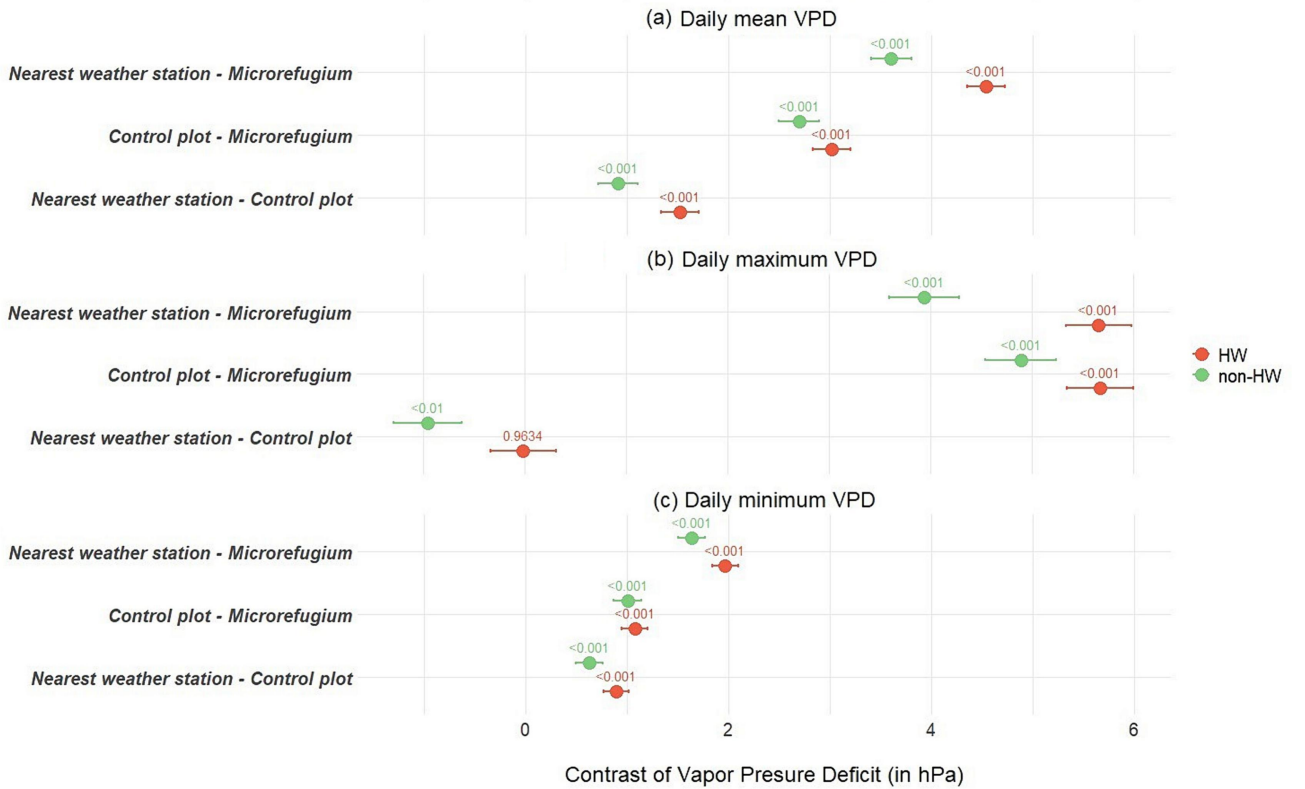
(a) Daily mean VPD
Nearest weather station - Microrefugium
Control plot - Microrefugium
Nearest weather station - Control plot
<0.001
<0.001
<0.001
<0.001
<0.001
<0.001
(b) Daily maximum VPD
Nearest weather station - Microrefugium
Control plot - Microrefugium
Nearest weather station - Control plot
<0.001
<0.001
<0.001
<0.001
<0.01
0.9634
HW
non-HW
(c) Daily minimum VPD
Nearest weather station - Microrefugium
Control plot - Microrefugium
Nearest weather station - Control plot
<0.001
<0.001
<0.001
<0.001
<0.001
<0.001
0
2
4
6
Contrast of Vapor Presure Deficit (in hPa)

Figure 6

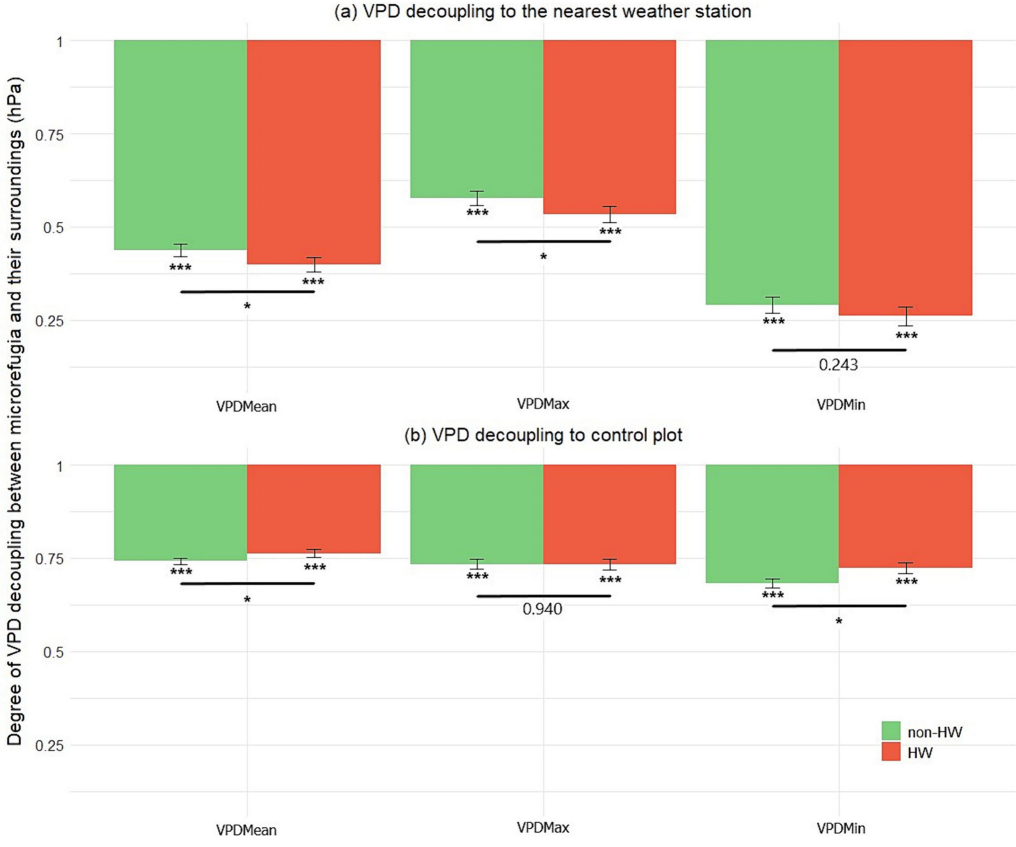
(a) VPD decoupling to the nearest weather station
(b) VPD decoupling to control plot
Degree of VPD decoupling between microrefugia and their surroundings (hPa)
1
0.75
0.5
0.25
***
*
0.243
0.940
VPDMean
VPDMax
VPDMin
non-HW
HW

Figure 7